Supporting Information

Structural Requirements of HDAC inhibitors: SAHA Analogues Modified at the C2 Position Display HDAC6/8 Selectivity

*Ahmed T. Negmeldin, Geetha Padige, Anton V. Bieliauskas, Mary Kay H. Pflum**

Department of Chemistry, Wayne State University, 5101 Cass Avenue, Detroit, Michigan 48202

Table of Contents

I. Experimental Procedures

I.A. Materials and Instrumentation

Unless otherwise noted, all organic synthesis was carried out under inert argon atmosphere in flame-dried glassware. “Iron-free” glassware was prepared by soaking glass vessels in a 6 M HCl acid bath overnight. “Iron-free” silica gel was prepared by washing with aqueous 6 M HCl until colorless, followed by washing with distilled water, and subsequently drying under air. Tetrahydrofuran (THF) was freshly distilled before use from sodium benzophenone ketyl. Dichlormethane (CH_2Cl_2) was freshly distilled before use from CaH_2, and triethylamine was freshly distilled before use from CaH_2. Flash chromatography was carried out using 60 Å, 230-400 mesh silica gel. Anhydrous methyl sulfoxide (DMSO) under AcroSeal^{TM}, ε-caprolactone, anhydrous lithium chloride (LiCl), sodium hydride, aniline, trimethylaluminum (2.0M solution in hexanes) and both alkyl halides were purchased from Acros Organics, Fisher Scientific, or Sigma-Aldrich. NMR spectra were taken on a Varian 500MHz instrument. IR spectra were taken on a Jasco FT/IR – 4100. HRMS spectra were taken on a Waters GCT EI-TOF. Syringe filters used were 0.22 µm Millipore Millex Syringe Drive Filter Unit, PES express. HPLC analysis to assess the purity of final compounds was performed with a Waters 1525 Binary HPLC pump and Waters 2998 Photodiode Array detector. The separation was performed on a reverse phase HPLC analytical column (YMC America, 250 x 4.6 mmI.D, 4µm, 8 nm) using a gradient of 90% to 10% of buffer A over 30 minutes (buffer A = 0.1% HPLC grade trifluoroacetic acid (TFA) in water; buffer B = HPLC grade acetonitrile) at a flow rate of 1.0 mL/min at room temperature. The synthesized final compounds were found to be ≥99% pure (Figures S5 and S10). The enantiomeric excess (% ee) was determined with the same HPLC system but with chiral analytical column (Chiracel OD-H, 250 x 4.6 mmI.D), eluting with 10% isopropanol in hexanes at a flow rate of 0.5 mL/min at room temperature. Optical rotations were measured in Perkin Elmer 341 Polarimeter.

I.B. Synthesis procedures for 1h and ii

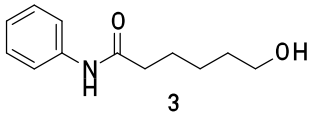

3

Synthesis of 5-hydroxy-N-phenylpentanamide (3). To a solution of ε-caprolactone **2** (1.1 mL, 10 mmol) in dry THF (100 mL) at 0°C was added trimethylaluminum (2.0 M solution in hexanes, 10 mL, 20 mmol) slowly. To this mixture, aniline (1.82 mL, 20 mmol) was added dropwise. The reaction mixture was stirred at room temperature for 1.5 hours. The reaction mixture was quenched by a slow addition of aqueous HCl (1 M) until evolution of gas was no longer observed, and stirring was continued for 30 minutes. The mixture was then diluted with H_2O (50 mL), extracted with Et_2O (4 x 100 mL), dried over magnesium sulfate, filtered and evaporated to an oil. Flash silica-gel chromatography (10-20% acetone in CH_2Cl_2) afforded a white solid (2.04 g, 98%). ^{1}H NMR (500MHz, $CDCl_3$) δ (ppm): 1.41 (m, 2H), 1.58 (m, 2H), 1.71 (m, 2H), 2.39 (m, 2H), 2.60 (bs, 1H), 3.59 (m, 2H), 7.10 (t, 1H), 7.29 (t, 2H), 7.59 (d, 2H), 7.90 (bs, 1H); ^{13}C NMR (125MHz, $CDCl_3$) δ (ppm): 25.8, 25.9, 32.1, 36.3, 61.9, 120.2, 124.1, 128.9, 138.8, 173.5; IR: 3297, 2936, 2862, 1663, 1598, 1543, 1498, 1442, 1309, 908, 729 cm^{-1}; HRMS (EI-TOF, m/z): found [M] 207.1259, calc. for $C_{12}H_{17}NO_2$, 207.1259.

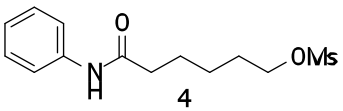

4

Synthesis of 6-oxo-6-(phenylamino) hexyl methanesulfonate (4). To a solution of **3** (2.04 g, 9.8 mmol) and triethylamine (1.8 mL, 12.7 mmol) in CH_2Cl_2 (25 mL) at 0°C was added methanesulfonyl chloride (0.91 mL, 11.8 mmol) and the reaction mixture was stirred at room temperature for 30 minutes. Aqueous HCl (1 M) was added to quench the reaction and stirring was continued for another 30 minutes. The mixture was then diluted with H_2O (50 mL), extracted with CH_2Cl_2 (4 x 100 mL), dried over magnesium sulfate, filtered, and adsorbed onto SiO_2. Dry-loaded flash silica gel chromatography (0-10% acetone in CH_2Cl_2) afforded a white solid (2.72 g 97%).^{1}H NMR (500 MHz, $CDCl_3$) δ (ppm): 1.49 (m, 2H), 1.79 (m, 4H), 2.38 (m, 2H), 2.9 (s, 3H), 4.20 (m, 2H), 7.10 (t, 1H), 7.30 (t, 2H), 7.50 (d, 2H), 7.60 (bs, 1H); ^{13}C NMR (125MHz, $CDCl_3$) δ (ppm): 25.5, 25.6, 29.0, 37.5, 37.6, 70.1, 120.1, 124.5, 129.1, 138.5, 171.5; IR: 3306, 2939, 1663, 1598, 1538, 1344, 1441, 1170, 945, 758 cm^{-1}. HRMS (ESI-LC–MS, **m/z**); found: [M+H], 286.1127, calculated for $C_{13}H_{20}NO_4S$, 286.1113, found: [M+Na], 308.0936, calculated for $C_{13}H_{19}NO_4Na$, 308.0932.

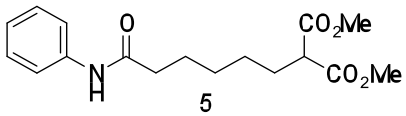

5

Synthesis of dimethyl 2-(6-oxo-6-(phenylamino)hexyl)malonate (5). To a slurry of NaH (60% dispersion in mineral oil, 0.6 g, 15 mmol) in dry THF (40 mL) at 0°C was added dimethyl malonate (1.7 mL, 15 mmol). The slurry was stirred at 0°C until clear (~30 minutes), before 6-oxo-6-(phenylamino) hexyl methanesulfonate **4** (1.43 g, 5.0 mmol) was added to the solution as a solid. The reaction mixture was then stirred at reflux for 20 hours. An aqueous solution of sat. $NaHCO_3$ (10 mL) was added to quench the reaction and stirring was continued for 30 minutes. The mixture was then diluted with H_2O (100 mL), extracted with Et_2O (4 x 100 mL), dried over magnesium sulfate, filtered, and evaporated to an oil. Flash silica-gel chromatography (50-70% Et_2O in petroleum ether) afforded **5** as white solid (1.46 g, 91%). ^{1}HNMR (500 MHz, $CDCl_3$) δ (ppm): 1.39 (m, 4H), 1.70 (m, 2H), 1.90 (m, 2H), 2.30 (m, 2H), 2.39 (m, 1H), 3.70 (s, 6H), 7.10 (t, 1H), 7.30 (t, 2H), 7.50 (m, 3H). ^{13}CNMR (125 MHz, $CDCl_3$) δ (ppm): 25.9, 27.5, 28.9, 29.1, 37.9, 52.0, 53.0, 73.9, 120.1, 124.5, 129.1, 138.5, 171.5, 172.0; IR: 3307, 2951, 1732, 1663, 1598, 1539, 1440, 756 cm^{-1}. HRMS (ESI-LC–MS, **m/z**); found: [M+H], 322.1664, calculated for $C_{17}H_{24}NO_5$, 322.1576, found: [M+Na], 344.1481, calculated for $C_{17}H_{23}NO_5Na$, 344.1474.

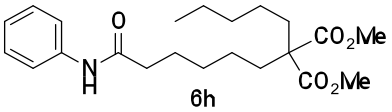

6h

Synthesis of dimethyl 2-(6-oxo-6-(phenylamino)hexyl)-2-pentylpropanedioate (6h). To a slurry of NaH (60% dispersion in mineral oil, 0.1 g, 2.8 mmol) in dry THF (0.1 M solution based on diester) at 0°C was added compound **5** (0.85 g, 2.2 mmol) as a solid. The slurry was stirred at 0°C until clear (~30 minutes), before addition of 1-bromopentane (0.42 mL, 3.27 mmol) at room temperature. The reaction mixture was then stirred at reflux for 3.5 hours. An aqueous solution of sat. $NaHCO_3$ (10mL) was added to quench the reaction and stirring was continued for 30 minutes. The mixture was then diluted with H_2O (100mL), extracted with Et_2O (4 x equal volume of aqueous

layer), dried over magnesium sulfate, filtered, and evaporated to an oil. Flash silica-gel chromatography (50-60% ether in petroleum ether) yielded the product **6h** as a clear oil (0.35 g, 41%). ^{1}HNMR (400 MHz, $CDCl_3$) δ (ppm): 0.90 (t, 3H), 1.10-1.4 (m, 10H), 1.7 (m, 2H), 1.9 (m, 4H), 2.3 (t, 2H), 3.7 (s, 6H), 7.1 (t, 1H), 7.3 (m, 3H), 7.5 (d, 2H); ^{13}CNMR (100 MHz, $CDCl_3$) δ (ppm): 15.2, 22.6, 24.0, 24.2, 27.5, 29.5, 32.2, 32.6, 32.8, 37.8, 52.0 (2), 58.0, 120.0, 124.0, 129.0, 138.0, 171.5, 172.5. IR: 3312, 2952, 2860, 1730, 1663, 1599, 1539, 1499, 1441, 1249, 754 cm^{-1}. HRMS (ESI-LC–MS, **m/z**); found: [M+H], 392.2444, calculated for $C_{22}H_{34}NO_5$, 392.2437, found: [M+Na], 414.2255, calculated for $C_{22}H_{33}NO_5Na$, 414.2256.

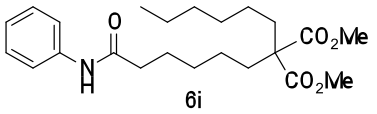

6i

Synthesis of dimethyl 2-hexyl-2-(6-oxo-6-(phenylamino) hexyl) propanedioate (6i). The procedure for **6h** was followed, but yielding 0.3370 g (38% yield) from 1-bromohexane (0.46 mL, 3.27 mmol). ^{1}HNMR (500 MHz, $CDCl_3$) δ (ppm): 0.90 (t, 3H), 1.10-1.30 (m, 10H), 1.40 (t, 2H), 1.75 (t, 2H), 1.90 (m, 4H), 2.35 (t, 2H), 3.70 (s, 6H), 7.1 (t, 1H), 7.3 (t, 2H), 7.45 (s, 1H), 7.5 (d, 2H); ^{13}CNMR (125 MHz, CDCl3) δ (ppm): 14.3, 22.8, 24.15, 24.3, 25.6, 29.6, 29.7, 31.8, 32.7, 32.95, 37.8, 52.5, 58.0, 120.0, 124.0, 129.0, 138.5, 171.5, 173.0; IR: 3306, 2952, 2857, 1731, 1663, 1599, 1540, 1499, 1441, 1244, 754 cm-1. HRMS (ESI-LC–MS, **m/z**); found: [M+H], 406.2594, calculated for $C_{23}H_{36}NO_5$, 406.2593, found: [M+Na], 428.2407, calculated for $C_{23}H_{35}NO_5Na$, 428.2413.

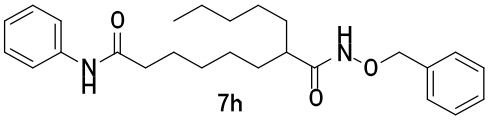

7h

Synthesis of N^{1}-(benzyloxy)-2-pentyl-N^{8}-phenyloctanediamide (7h). To compound **6h** (0.35 g, 0.89 mmol) was added DMSO to make a 0.1 M solution. LiCl (0.08 g, 1.8 mmol) was added to the solution, followed by H_2O (0.03 g, 1.8 mmol). The mixture was warmed to reflux and stirred 3.5 hours. The reaction mixture was quenched with an aqueous solution of sat. $NaHCO_3$ (20mL), transferred to a separatory funnel, and extracted with dichloromethane (50mL). The organic layers were pooled, dried over magnesium sulfate, filtered, and evaporated to oil.

Without any further purification, the oil was dissolved in MeOH (0.1 M solution based on diester **6h**). NaOH (0.7 g, 18 mmol) was added as a 5 M aqueous solution via syringe. The mixture was warmed to reflux and stirred 5 hours. The reaction mixture was quenched by addition of concentrated HCl until acidic, as monitored with pH paper. The mixture was then transferred to a separatory funnel and extracted with ethyl acetate. The organic layers were pooled, dried over magnesium sulfate, filtered, and evaporated to an oil. Flash silica-gel chromatography (50% ethyl acetate in hexanes) gave the intermediate acid product as an off-white solid.

O-benzylhydroxylamine hydrochloride (0.14 g, 0.9 mmol) was dissolved in a minimal amount of water and added to a separatory funnel followed by addition of Na_2CO_3 (0.05 g, 0.45 mmol) dissolved in a minimal amount of water. The separatory funnel was shaken vigorously until gas evolution was no longer observed (about 10 min). The mixture was then extracted with diethyl ether (four times with an equal volume to aqueous layer). The organic layers were pooled, dried over magnesium sulfate, filtered, and evaporated to an oil. In a separate flask, carbonyldiimidazole (CDI) (0.12 g, 0.75 mmol) was added to a solution of the acid intermediate from the last step (0.19 g, 0.60 mmol) in THF (6 mL, 0.1 M solution based on the acid intermediate) followed by triethylamine (TEA) (0.16 mL, 1.2 mmol). The hydroxylamine oil was subsequently added in four portions to the flask containing the activated

carboxylic acid. The mixture was refluxed overnight. The reaction was quenched with aqueous HCl (1 M) and extracted with diethyl ether (four times with an equal volume to aqueous layer). The organic layers were pooled, dried over magnesium sulfate, filtered, and evaporated to an oil. Flash silica-gel chromatography (10% acetone in CH_2Cl_2) gave the product **7h** as a white solid (0.1431 g, 38% yield over the three steps). ^{1}HNMR (400 MHz, CD_3OD) δ (ppm): 0.90 (t, 3H), 1.15-1.40 (m, 12H), 1.60 (m, 4H), 1.90 (m, 1H), 2.3 (t, 2H), 4.90 (s, 2H), 7.1 (t, 1H), 7.2-7.4 (m, 7H), 7.5 (d, 2H), 8.0, (bs, 1H), 9.0 (bs, 1H); ^{13}CNMR (100 MHz, $CDCl_3$) δ (ppm): 15.0, 22.5, 26.0, 27.0, 28.0, 29.0, 32.5, 33.0, 33.5, 38.0, 44.5, 79.0, 121.0, 124.3, 128.75, 128.85, 129.1, 129.5, 135.6, 138.5, 172.0, 174.0; IR: 3194, 2929, 2856, 1654, 1598, 1542, 1498, 1442, 1309, 1252, 752 cm$^-$1; HRMS (EI-TOF, **m/z**): found [M], 424.2716, calculated for $C_{26}H_{36}N_2O_3$, 424.2726.

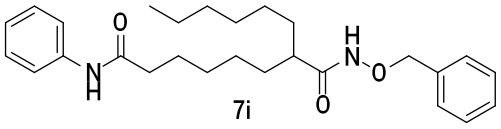

7i

Synthesis of N^1-(benzyloxy)-2-hexyl-N^8-phenyloctanediamide (7i). The procedure for **7h** was followed, but yielding 0.1976 g (54% yield over the three steps) from **6i** (0.3370 g, 0.83 mmol). ^{1}HNMR (500 MHz, CD_3OD) δ (ppm): 0.9 (t, 3H), 1.2-1.4 (m, 14H), 1.55 (m, 2H), 1.65 (m, 2H), 1.95 (m, 1H), 2.3 (t, 2H), 4.85 (s, 2H), 7.1 (t, 1H), 7.3-7.4 (m, 7H), 7.5 (d, 2H); ^{13}CNMR (125 MHz, CD_3OD) δ (ppm): 13.0, 22.5, 24.5, 27.5, 27.6, 28.5, 29.0, 31.8, 32.3, 32.5, 37.0, 43.5, 77.5, 120.5, 123.9, 128.3, 128.4, 128.6, 129.1, 136.0, 139.0, 173.0, 174.5; HRMS (EI-TOF, **m/z**): found [M], 438.2884, calculated for $C_{27}H_{38}N_2O_3$, 438.2882.

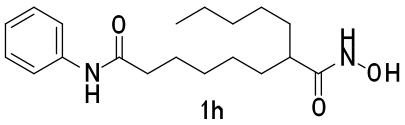

1h

Synthesis of N^1-hydroxy-2-pentyl-N^8-phenyloctanediamide (1h). To a flask containing **7h** (0.1400 g, 0.33 mmol), methanol (3 mL, to make a 0.1 M solution) and 10% palladium on carbon (0.003 g, 0.033 mmol) were added. The flask was vacuum purged with argon several times, followed by hydrogen several times. The reaction was allowed to stir under hydrogen pressure for 3 hours. The mixture was filtered through a celite pad into an acid-washed flask and the precipitate was rinsed with methanol. Hot filtration to remove residual celite into an acid-washed flask afforded the product **1h** as a white solid (0.0583 g, 53%). The compound was further purified by HPLC on a reverse phase HPLC semi-preparative column (YMC America, 250 x 10 mmI.D., 4μm, 8 nm) using a gradient of 90% to 10% of buffer A over 90 minutes (buffer A = 0.1% HPLC grade TFA in water; buffer B = HPLC grade acetonitrile) at a flow rate of 3.0 mL/min at room temperature. ^{1}HNMR (500 MHz, CD_3OD) δ (ppm): 0.9 (t, 3H), 1.2-1.4 (m, 12H), 1.55 (m, 2H), 1.7 (t, 2H), 2.0 (m, 1H), 2.35 (t, 2H), 7.1 (t, 1H), 7.3 (t, 2H), 7.5 (d, 2H); ^{13}CNMR (125 MHz, CD_3OD) δ (ppm): 17.0, 22.0, 25.5, 26.5, 26.7, 29.0, 32.0, 33.0, 33.2, 37.0, 44.0, 120.0, 124.0, 128.5, 138.5, 173.5, 174.5; IR: 3247, 2928, 2857, 1645, 1544, 1499, 1442 cm^{-1}; HRMS (EI-TOF, *m/z*): found [M-H2O], 316.2148, calculated for $C_{19}H_{28}N_2O_2$, 316.2151.

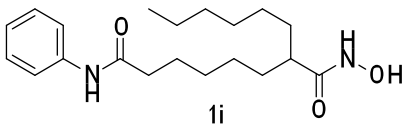

1i

Synthesis of 2-hexyl-N^1-hydroxy-N^8-phenyloctanediamide (1i). The procedure for **1h** was followed, but yielding 0.1145 g (76% yield) from *N*1-(benzyloxy)-2-hexyl-*N*8-phenyloctanediamide **7i** (0.1900 g, 0.43 mmol). The compound was further purified by HPLC as described for 1h, except a gradient of 60% to 10% of buffer A over 90 minutes was used. ^{1}HNMR (300 MHz, CD_3OD) δ (ppm): 0.90 (t, 3H), 1.2-1.45 (m, 14H), 1.6-1.7 (m, 4H), 2.0 (m, 1H), 2.35 (t, 2H), 7.1 (t, 1H), 7.3 (t, 2H), 7.5 (d, 2H); ^{13}CNMR (75 MHz, CD_3OD) δ (ppm): 13.0, 23.0, 25.5, 27.0, 27.5, 29.0, 29.3, 32.0, 33.0, 33.2, 37.0, 44.0, 120.0, 124.0, 128.5, 139.0, 173.5, 174.5; IR: 3248, 2927, 2855, 1642, 1543, 1499, 1418, 1309, 754 cm^{-1}; HRMS (EI-TOF, *m*/*z*): found [M], 348.2423, calculated for $C_{20}H_{32}N_2O_3$, 348.2413.

I.C. Synthesis procedures for (*S*)-1i and *(R)*-1i

The synthetic Scheme to generate **(*S*)-1i** is shown in Scheme 2 of the manuscript. The synthesis of (***R***)**-1i** is show below.

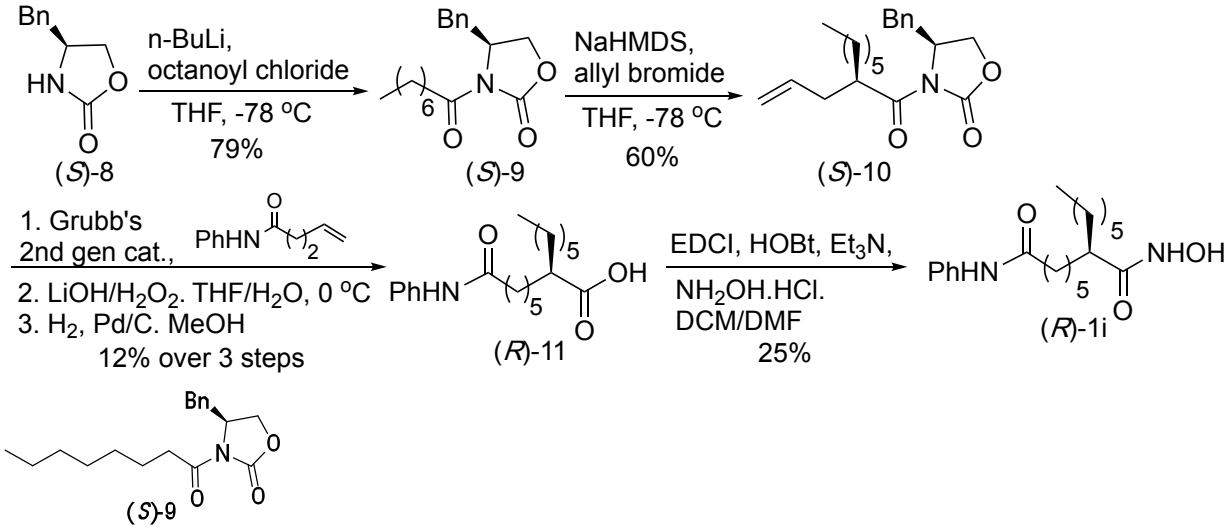

Synthesis of (*S*)-4-benzyl-3-octanoyloxazolidin-2-one ((*S*)-9). The compound was synthesized according to the reported procedure.[1] Briefly, **(S)-8** (1.44 g, 8.15 mmol) was dissolved in dry THF (25 mL) followed by the addition of butyl lithium (3.26 mL of 2.5 M solution, 8.16 mmol) drop wise under argon at -78°C. The reaction was stirred at that temperature for 10 minutes, then octanoyl chloride (1.53 mL, 8.96 mmol) was added drop wise. Stirring was continued for 30 minutes at -78°C, then the reactino temperature was raised to gradually room temperature over 30 minutes. The reaction was diluted with saturated solution of ammonium chloride (30 mL). THF was evaporated at reduced pressure and the reaction was extracted with ethyl acetate (2 x 30 mL). The organic extracts were then evaporated and the product was purified by Flash silica-gel chromatography (5-10% ethyl acetate in hexanes) yielded the product **(S)-9** (1.95 g, 79%). ^{1}HNMR (400 MHz, $CDCl_3$) δ (ppm): 0.88 (t, 3H), 1.34 (m, 8H), 1.68 (m, 2H), 2.75 (dd, 2H), 2.93 (m, 2H), 3.29 (dd, 1H), 4.18 (m, 2H), 4.66 (m, 1H), 7.21 (d, 2H), 7.27 (m, 1H), 7.33 (t, 2H); ^{13}CNMR (100 MHz, $CDCl_3$) δ (ppm): 14.09, 22.62, 24.26, 29.06, 29.09, 31.69, 35.54, 37.92, 55.15, 66.14, 127.33, 128.95, 129.42, 135.33, 153.46, 173.46. LRMS (LC-SQMS, **m/z**); found: [M+H], 304.04, calculated for $C_{18}H_{26}NO_3$, 304.18, found: [M+Na], 326.01, calculated for $C_{18}H_{25}NO_3Na$, 326.17.

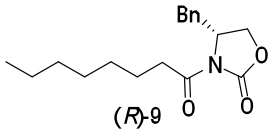

(*R*)-9

Synthesis of (*R*)-4-benzyl-3-octanoyloxazolidin-2-one ((*R*)-9). The procedure for **(S)-9** was followed, but yielding 2.18 g (84% yield) from **(R)-8** (1.5 g, 8.47 mmol). ^{1}HNMR (400 MHz, $CDCl_3$) δ (ppm): 0.90 (t, 3H), 1.30 (m, 8H), 1.68 (m, 2H), 2.76 (dd, 2H), 2.91 (m, 2H), 3.29 (dd, 1H), 4.16 (m, 2H), 4.66 (m, 1H), 7.2 (d, 2H), 7.27 (m, 1H), 7.33 (t, 2H); ^{13}CNMR (100 MHz, $CDCl_3$) δ (ppm): 14.1, 22.62, 24.26, 29.06, 29.09, 31.69, 35.54, 37.92, 55.15, 66.14, 127.32, 128.94, 129.42, 135.33, 153.46, 173.44. LRMS (LC-SQMS, **m/z**); found: [M+H], 304.08, calculated for $C_{18}H_{26}NO_3$, 304.18, found: [M+Na], 325.99, calculated for $C_{18}H_{25}NO_3Na$, 326.17.

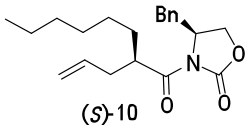

(*S*)-10

Synthesis of (*S*)-3-((*R*)-2-allyloctanoyl)-4-benzyloxazolidin-2-one ((*S*)-10). To compound **(S)-9** (1.95 g, 6.43 mmol) was added dry THF (25 mL) followed by reduction of the temperature to -78°C. Sodium bis(trimethylsilyl)amide (NaHMDS, 3.53 mL of 2 M solution, 7.07 mmol) was added drop wise under Argon and the reaction was stirred at -78°C for 1 hour. Allyl bromide (1.65 mL, 19.28 mmol) was then added drop wise, and the reaction was stirred at -78°C for 45 minutes, then the temperature was increased gradually to 0°C and stirring was continued for 1 hour at 0°C. The reaction was then quenched with saturated ammonium chloride solution (30 mL) and was left to stir at room temperature for 15 minutes. The reaction was concentrated under reduced pressure, and the aqueous layer was extracted with ethyl acetate (3 x 30 mL). The extracts were evaporated and the product was purified by flash silica-gel chromatography (3% ethyl acetate in hexanes), which yielded the product **(S)-10** (1.32 g, 60%). ^{1}HNMR (400 MHz, $CDCl_3$) δ (ppm): 0.87 (t, 3H), 1.27 (m, 8H), 1.49 (m, 1H), 1.7 (m, 1H), 2.32 (m, 1H), 2.47 (m, 1H), 2.65 (dd, 1H), 3.31 (dd, 1H), 3.91 (m, 1H), 4.16 (m, 2H), 4.66 (m, 1H), 5.05 (dd, 2H), 5.82 (m, 1H), 7.26 (m, 5H); ^{13}CNMR (100 MHz, $CDCl_3$) δ (ppm): 14.06, 22.58, 27.21, 29.34, 31.58, 31.66, 36.81, 38.11, 42.32, 55.53, 65.90, 117.09, 127.29, 128.93, 129.42, 135.33, 135.46, 153.16, 176.15. LRMS (LC-SQMS, **m/z**); found: [M+H], 344.04, calculated for $C_{21}H_{30}NO_3$, 344.21, found: [M+Na], 365.99, calculated for $C_{21}H_{29}NO_3Na$, 366.20. $[\alpha]_D^{23}$ = +74.5 (*c* .76, CH_2Cl_2).

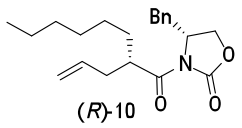

(*R*)-10

Synthesis of (*R*)-3-((*S*)-2-allyloctanoyl)-4-benzyloxazolidin-2-one ((*R*)-10). The procedure for **(S)-10** was followed, but yielding 1.56 g (64% yield) from **(R)-9** (2.15 g, 7.08 mmol). ^{1}HNMR (400 MHz, $CDCl_3$) δ (ppm): 0.87 (t, 3H), 1.27 (m, 8H), 1.49 (m, 1H), 1.72 (m, 1H), 2.32 (m, 1H), 2.45 (m, 1H), 2.66 (dd, 1H), 3.29 (dd, 1H), 3.91 (m, 1H), 4.15 (m, 2H), 4.68 (m, 1H), 5.06 (m, 2H), 5.82 (m, 1H), 7.27 (m, 5H); ^{13}CNMR (100 MHz, $CDCl_3$) δ (ppm): 14.06, 22.58, 27.20, 29.34, 31.58, 31.66, 36.80, 38.11, 42.32, 55.53, 65.89, 117.09, 127.29, 128.93, 129.41, 135.32, 135.46, 153.15, 176.15. LRMS (LC-SQMS, **m/z**); found: [M+H], 344.02, calculated for $C_{21}H_{30}NO_3$, 344.21, found: [M+Na], 366.02, calculated for $C_{21}H_{29}NO_3Na$, 366.20. $[\alpha]_D^{23}$ = –70.7 (*c* 0.49, CH_2Cl_2).

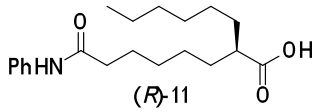

(*R*)-11

Synthesis of (*R*)-2-hexyl-8-oxo-8-(phenylamino)octanoic acid ((*R*)-11). To a solution of **(S)-10** (1.32 g, 3.84 mmol) in dichloromethane (DCM, 30 mL) was added *N*-phenylpent-4-enamide (2.69 g, 15.36 mmol) and Grubb's second generation catalyst (261 mg, 8 mol%). The reaction was heated at 50°C for 12 hours. The solvent was evaporated. Flash silica-gel chromatography (1:6 to 1:4 ethyl acetate in hexanes) yielded the alkene intermediate (904 mg, 48%). The intermediate was used in the following reaction with no characterization.

The intermediate alkene (451 mg, 0.92 mmol) was dissolved in a mixture of THF (20 mL) and water (5 mL). Hydrogen peroxide (0.42 mL of 30% solution, 3.68 mmol) was added at 0°C, followed by lithium hydroxide monohydrate (78 mg, 1.86 mmol) dissolved in 3 mL water. The reaction was stirred at 0°C for 6 hours, then sodium sulfite (1 g) in 7 mL water was added. The reaction was stirred for additional 15 minutes at room temperature. The reaction was diluted with 10% HCl to pH 2, and then extracted with ethyl acetate (2 x 40 mL). The extracts were evaporated and the crude product was used in the next reaction.

The crude product was dissolved in methanol (15 mL), then 20% Pd/C was added (22 mg, 10% w/w). Air was replaced with argon (x3) then with hydrogen gas (3x). The reaction was left to stir under hydrogen overnight. The reaction was then filtered and the product was purified by flash silica-gel chromatography (1:6 to 1:2 ethyl acetate in hexanes), which yielded the product **(R)-11** (212 mg, 69% over 2 steps). ^{1}HNMR (400 MHz, $CDCl_3$) δ (ppm): 0.87 (t, 3H), 1.28 (m, 14H), 1.68 (m ,4H), 2.32 (m, 3H), 7.08 (t, 1H), 7.27 (m, 2H), 7.52 (m, 3H); ^{13}CNMR (100 MHz, $CDCl_3$) δ (ppm): 14.06, 22.59, 25.42, 26.98, 27.34, 28.95, 29.20, 31.65, 31.88, 32.31, 37.14, 45.49, 119.91, 124.22, 128.95, 137.91, 171.66, 182.08. LRMS (LC-SQMS, **m/z**); found: [M+H], 334.16, calculated for $C_{20}H_{32}NO_3$, 334.23, found: [M+Na], 355.99, calculated for $C_{20}H_{31}NO_3Na$, 356.22, found: [M-H], 332.22, calculated for $C_{20}H_{30}NO_3$, 332.23.

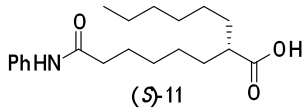

(*S*)-11

Synthesis of (*S*)-2-hexyl-8-oxo-8-(phenylamino)octanoic acid ((*S*)-11). The procedure for **(R)-11** was followed, but yielding 922 mg (43% yield) for the cross metathesis reaction from **(R)-10** (1.5 g, 4.4 mmol), and then 174 mg (28% over 2 steps) of **(S)-11**. ^{1}HNMR (400 MHz, $CDCl_3$) δ (ppm): 0.87 (t, 3H), 1.43 (m, 14H), 1.64 (m ,4H), 2.33 (m, 3H), 7.09 (t, 1H), 7.30 (m, 3H), 7.51 (d, 2H); ^{13}CNMR (100 MHz, $CDCl_3$) δ (ppm): 14.06, 22.59, 25.39, 26.97, 27.33, 28.94, 29.19, 31.64, 31.96, 32.29, 37.55, 45.39, 119.92, 124.22, 128.97, 137.91, 171.47, 181.79. LRMS (LC-SQMS, **m/z**); found: [M-H], 332.13, calculated for $C_{20}H_{30}NO_3$, 332.23.

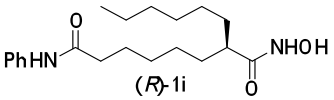

(*R*)-1i

Synthesis of (*R*)-2-hexyl-*N*^{1}-hydroxy-*N*^{8}-phenyloctanediamide ((*R*)-1i). In an acid washed flask, carboxylic acid **(R)-11** (295 mg, 0.87 mmol) was dissolved in dry DCM (20 mL), followed by the addition of triethylamine (247 uL, 1.77 mmol), hydroxybenzotriazole (HOBt, 204 mg, 1.33 mmol) and N-(3-dimethylaminopropyl)-N′-ethylcarbodiimide hydrochloride (EDCI HCl, 272 mg, 1.42 mmol). The reaction was stirred for 1 hour, then triethyl amine (618 uL, 4.43 mmol), hydroxyl

amine HCl (308 mg, 4.43 mmol) and DMF (5 mL) were added. The reaction was stirred overnight. The reaction was then concentrated under reduced pressure, diluted with distilled deionized water, and extracted with ethyl acetate (2 x 30 mL). The product was purified by Flash silica-gel chromatography (2% methanol in DCM, then 1:8 to 1:4 acetone in DCM) yielded the product **(R)-1i** (30 mg, 10%). ^{1}HNMR (400 MHz, CD_3OD) δ (ppm): 0.89 (t, 3H), 1.35 (m, 14H), 1.67 (m, 4H), 2.02 (m, 1H), 2.35 (t, 2H), 7.07 (t, 1H), 7.28 (t, 2H), 7.52 (d, 2H); ^{13}CNMR (100 MHz, CD_3OD) δ (ppm): 13.00, 22.23, 25.34, 26.83, 27.14, 28.75, 28.94, 31.50, 32.28, 32.48, 36.43, 43.58, 119.84, 123.70, 128.34, 138.46, 173.24, 173.98; HRMS (Waters LCT-MS premier TOF, *m*/*z*): found [M+Na], 371.2313, calculated for $C_{20}H_{32}N_2O_3Na$, 371.2311. $[\alpha]_D^{23}$ = −1.74 (*c* 0.3, EtOH). Chiral HPLC: 92% ee.

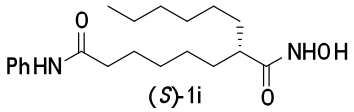

(*S*)-1i

Synthesis of (*S*)-2-hexyl-*N*^{1}-hydroxy-*N*^{8}-phenyloctanediamide ((*S*)-1i). The procedure for **(R)-1i** was followed, but yielding 30 mg (25% yield) from **(S)-11** (116 mg 0.35 mmol). ^{1}HNMR (400 MHz, CD_3OD) δ (ppm): 0.88 (t, 3H), 1.34 (m, 14H), 1.64 (m, 4H), 2.02 (m, 1H), 2.35 (t, 2H), 7.07 (t, 1H), 7.28 (t, 2H), 7.53 (d, 2H); ^{13}CNMR (100 MHz, CD_3OD) δ (ppm): 13.02, 22.24, 25.35, 26.84, 27.15, 28.76, 28.95, 31.51, 32.29, 32.49, 36.44, 43.58, 119.85, 123.71,128.35, 138.46, 173.24, 173.98; HRMS (Waters LCT-MS premier TOF, *m*/*z*): found [M+Na], 371.2320, calculated for $C_{20}H_{32}N_2O_3Na$, 371.2311. $[\alpha]_D^{23}$ = +1.45 (*c* 0.9, EtOH). Chiral HPLC: 95% ee.

I.D. Procedures for biological screenings

I.C.1. HeLa cell lysis. HeLa-S3 cells (purchased from ATCC) were lysed in lysis buffer (1 x 10^9 cells in 9mL lysis buffer; 50mM Tris-HCl, pH 8.0, 10% glycerol, 150mM NaCl, 0.5% Triton X-100) containing Calbiochem protease inhibitor cocktail set V with rotation at 4 °C for 30 min. Cell debris was removed by centrifugation at 12000 rpm at 4 °C for 30 min. Protein concentration of the supernatant was determined using Bio-Rad protein assay (BioRad, Bradford reagent).

I.D.2. Inhibitors testing with HDAC isoforms. Screening with HDAC1, 2, 3, and 6 was performed according to the reported procedure.[2] Briefly, individual wells of a high binding polystyrene 96-well white opaque plate (Thermo Scientific) were incubated in binding buffer (100 µL; 0.2M carbonate/0.2M bicarbonate buffer, pH 9.4) containing primary HDAC1 antibody (Sigma Aldrich, H3284, 100µL of 10µg/mL), primary HDAC2 antibody (Sigma Aldrich, H3159, 100µL of 10µg/mL), or primary HDAC6 antibody (Sigma Aldrich, SAB1404771, 100µL of 2µg/mL) with rocking (3 rpm) for 1 hr at room temperature, or at 4°C overnight with no rocking. For HDAC3 with compounds **1g-i,** primary HDAC3 antibody (Sigma Aldrich, H3034, 100µL of 25µg/mL) was used following the same procedure described above. But in the case of HDAC3 with all other compounds, wells of a secondary antibody coated 96-well white opaque plate (G-Biosciences) were incubated with primary HDAC3 antibody (Sigma Aldrich, H3034, 100µL of 1µg/mL) in TBST buffer (50mM Tris-HCl, 150 mM NaCl, pH 7.4, 0.05% (v/v) Tween-20) containing 0.1% (w/v) bovine serum albumin (BSA, Jackson Immunoresearch) at 4°C overnight without rocking. For all reactions, unbound antibody was removed by washing quickly three times with TBST buffer (300µL), followed by a fourth wash with TBST (300 µL) with 5 minutes incubation and rocking (3 rpm) at room temperature. In the case of high binding

polystyrene plates containing HDAC1, 2, 3, or 6 antibodies, the unbound regions of the well were blocked with 5% non-fat dry milk in TBST buffer (300µL) for 1 hr at room temperature with rocking (3 rpm). Because the secondary antibody coated plates containing HDAC3 were pre-blocked by the manufacturer, no additional blocking step was included.

To affix HDAC enzyme to the plate, HeLa cell lysates (100µL of 100µg/mL for HDAC1, 2, and 3 and 100µL of 1 mg/mL for HDAC6 in TBST buffer containing 0.1 % (w/v) non-fat dry milk) were added to each well and incubated for 1 h at 4°C without rocking, followed by washing with TBST, as described previously. For HDAC3 with compounds **1g-i** only, HeLa cell lysates (100µL of 1 mg/mL in TBST buffer containing 0.1 % (w/v) non-fat dry milk) were used, followed by incubation and washing as described earlier. Inhibitors in DMSO (1 µL) were mixed with HDAC-Glo™ buffer (24 µL), then added to the plate and incubated for 15 min at room temperature without rocking. An uninhibited control reaction was also included that contained DMSO (1 µL) in HDAC-Glo™ buffer (24 µL). Finally, deacetylase activity was measured using the HDAC-Glo™ assay kit (Promega) as per the manufacturer's protocol. Specifically, the HDAC-Glo™ substrate (1 mL) and developer (1 µL) were first premixed and stored at -20°C. Then, to monitor deacetylase activity, the HDAC-Glo™ reagents (25µL) were added to each well (50 µL total volume) and incubated for 30-45 min at room temperature without rocking. The deacetylase activity was measured as luminescent signal using a GeniosPlus Fluorimeter (Tecan) at optimal gain. The concentrations of inhibitors reported in the single dose screen (Figure 2) and dose-dependent studies are final concentrations after addition of HDAC-Glo™ reagent. For the single concentration screen, the percent deacetylase activity remaining was calculated by dividing the signal with inhibitor by the signal without inhibitor (DMSO negative control reaction), and then multiplying by 100. For dose-dependent reactions to determine IC_{50}, the luminescent signal was first background corrected with the signal from a negative control reaction where the HDAC antibody was absent in the initial antibody binding step before the percent deacetylase activity was calculated. The mean percent deacetylase activity along with standard error of three independent trials is reported in Figure 2.

Inhibitory activity with HDAC8 with all compounds was measured using the following procedure. In a half area 96-well plate, HDAC8 (75 ng, BPS Bioscience) was incubated in HDAC-Glo™ buffer (39 µL) with small molecule in DMSO (1 µL), or DMSO alone (1 µL) as a control, for 15 minutes at room temperature. HDAC-Glo™ reagent (10 µL) was added to each reaction and incubated for 15-30 min at room temperature. Luminescent signal was measured at 25-30 minutes after adding the substrate reagent using a Geniosplus Fluorimeter (Tecan) at optimal gain. To determine IC_{50}, the luminescent signal was first background corrected with the signal from a background control reaction where no HDAC8 enzyme was added.

IC_{50} values were calculated by fitting the percent deacetylase activity remaining as a function of inhibitor concentration to a sigmoidal dose-response curve ($y = 100/(1+(x/IC_{50})^z)$, where y = percent deacetylase activity and x = inhibitor concentration) using non-linear regression with KaleidaGraph 4.1.3 software (Tables 1, S3-S9, Figures S39-S45).

I.D.3. In cell target and selectivity validation

U937 cells were grown in RPMI media supplemented with 10% fetal calf serum and 1% penicillin/streptomycin under humidified conditions (37 °C, 5% CO_2). Cells were added (10^6 cells/well) to a 12 well plate in RPMI-1640 (no phenol red) media, supplemented with 10% fetal calf serum and 1% penicillin/streptomycin (990 µL final volume). The cells were treated with DMSO (10 µL) or the small molecule in DMSO (10 µL), and incubated for the 18 hours under humidified conditions (37 °C, 5% CO_2). The cells were then washed once with cold PBS (500 µL) and lysed with lysis buffer (20 µL) containing 1X protease inhibitor for 30 minutes at 0°C. The total protein concentration in the supernatant was then quantified using the Bradford assay kit (Bio-Rad) with BSA as the standard.

Equal quantities of proteins were mixed with BME (10% of the final volume) and SDS loading buffer (50 mM Tris-Cl [pH 6.8], 100 mM DTT, 2% SDS, 0.1% bromophenol blue, 10% glycerol) before the proteins were denatured at 95 °C for 3 minutes. The proteins in each sample were separated by 16% SDS-polyacrylamide gel electrophoresis (SDS-PAGE), then transferred to PVDF membrane (Immobilon P, Millipore). The membrane was blocked with 5% (w/v) nonfat milk in TBST buffer at room temperature for 1 h. The blocked membrane was incubated with a primary antibody (anti-GAPDH (Cell Signaling, 5174P); anti-Acetyl-α-tubulin(Lys40) (Cell Signaling, 5335P), or anti-Acetyl-histone H3(Lys9) (Cell Signaling, 9649P)) at a 1:1000 dilution in TBST buffer at 4 °C overnight. Finally, the membrane was incubated with HRP-conjugated goat anti-rabbit secondary antibody (Cell signaling, 7074S; 7:10000 dilution) at room temperature for 1 h. HRP activity was detected using an enhanced chemiluminescence light-based detection substrate, SuperSignal West Dura Extended Duration Substrate (ThermoFisher Scientific, 34075) and Alpha Innotech FluorChem imaging system. The western blots were quantified using AlphaView FluorChem 3.2.2 program. Statistical significance of compound effects was calculated using one way ANOVA and Tukey post-hoc test.

I.D.4. *In-vitro* cell growth inhibition

Jurkat, AML-MOLM-13, or U937 cells were grown in RPMI media supplemented with 10% fetal calf serum and 1% penicillin/streptomycin under humidified conditions (37°C, 5% CO_2). Cells were seeded in 96-well cell culture plates with a density of $4x10^4$ cells in 99 µL of media composed of RPMI-1640 (no phenol red), supplemented with 10% fetal calf serum and 1% penicillin/streptomycin. The cells were treated with 1 µM or 10 µM single concentrations or serial dilution (2-fold) of compounds **1g-i** in DMSO (1 µL). DMSO only was used in the no inhibitor control. A negative control was also included where no cells were added. The plate was incubated for 44 hours at 37 °C in humid 5% CO_2 atmosphere. A solution of 3-(4,5-dimethylthiazol-2-yl)-2,5-diphenyltetrazolium bromide (MTT, 10 µL of 5 mg/mL in DPBS buffer (HyClone™ Dulbecco's Phosphate Buffered Saline)) was added to each well. The cells were incubated for another 4 h at 37 °C in humid 5% CO_2 atmosphere for development to take place. The resulting purple formazan crystals were dissolved by addition of DMSO (150 µL), and the absorbance was measured at 595 nm using a Geniosplus Fluorimeter (Tecan). For all wells containing inhibitor, the signal was background corrected with the signal from a negative control reaction (media and MTT only) before the percent viable cells was calculated. The percent viable cells was calculated by dividing the absorbance with inhibitor by the absorbance without inhibitor (DMSO, cells, and MTT). The assay was performed at least three independent times. For the single concentrations experiment, the mean percent viable cells along with standard error of three independent trials is reported in Figure 4. EC_{50} values were calculated by fitting the percent viable cells as a function of inhibitor concentration to a sigmoidal dose-response curve ($y = 100/(1+(x/EC_{50})^z)$, where y = percent viable cells and x = inhibitor concentration) using non-linear regression with KaleidaGraph 4.1.3 software.

I.E. Docking procedure

The AutoDock 4.2 program[3-4] was used to perform the docking calculations. The HDAC2 crystal structure was downloaded from the protein data bank (pdb ID: 3MAX).[5] The PyMOL program was used to delete two chains and remove water molecules, metal ions (calcium and sodium), and the cocrystallized ligand in the active site from the crystal structure; only the zinc atoms remained. For HDAC2, a grid box of size 60 X 60 X 60 $Å^3$ with a spacing of 0.375 Å and centered at (69.643, 30.937, -0.989) was used. HDAC6 crystal structure was downloaded from protein databank. (pdb: 5EEM).[6] Pymol program was used to manually delete water molecules. A grid box of size 42 X 44 X

40 $Å^3$ with a spacing of 0.375 Å and centered at (7.000, 17.000, -22.000) was used. For both HDAC2 and HDAC6, AutoDockTools-1.5.4[4] was used to add all polar hydrogen atoms, compute Gasteiger charges, merge all nonpolar hydrogen, and generate pdbqt files. The charge of the zinc atom was manually changed from zero to +2. The map type was set by choosing the ligand and then AutoGrid 4.2 was used to pre-calculate and generate the grid map files required for the docking calculations. All the docked compounds were drawn in ChemBioDraw Ultra 12.0, and Chem 3D Pro 12.0 was used to run MM2 job for energy minimization. Then AutoDockTools-1.5.4 program was used to choose torsions, compute Gasteiger charges, and generate the pdbqt files. All acyclic bonds were made rotatable, except the amide bonds. The generated pdbqt file for the enzyme (or the homology model) was set as a rigid macromolecule and the genetic algorithm search parameters were set to 100 GA runs for each ligand with a population size of 150, a maximum number of 2.5×10^5 energy evaluations, a maximum number of 2.7×10^4 generations, a mutation rate of 0.2 and a crossover rate of 0.8. The docking parameters were set to default. All output DLG files were converted to pdbqt format and the results were visualized in PyMOL. Among the 100 docked poses generated, the ones shown in Figures 5, S50, S51 and S52 displayed optimal distances between the hydroxamic acid group of the inhibitor and the catalytic metal of the protein.

II. Compound characterization

Compound characterization of C2-*n*-pentyl SAHA (1h) and C2-*n*-hexyl SAHA (1i)

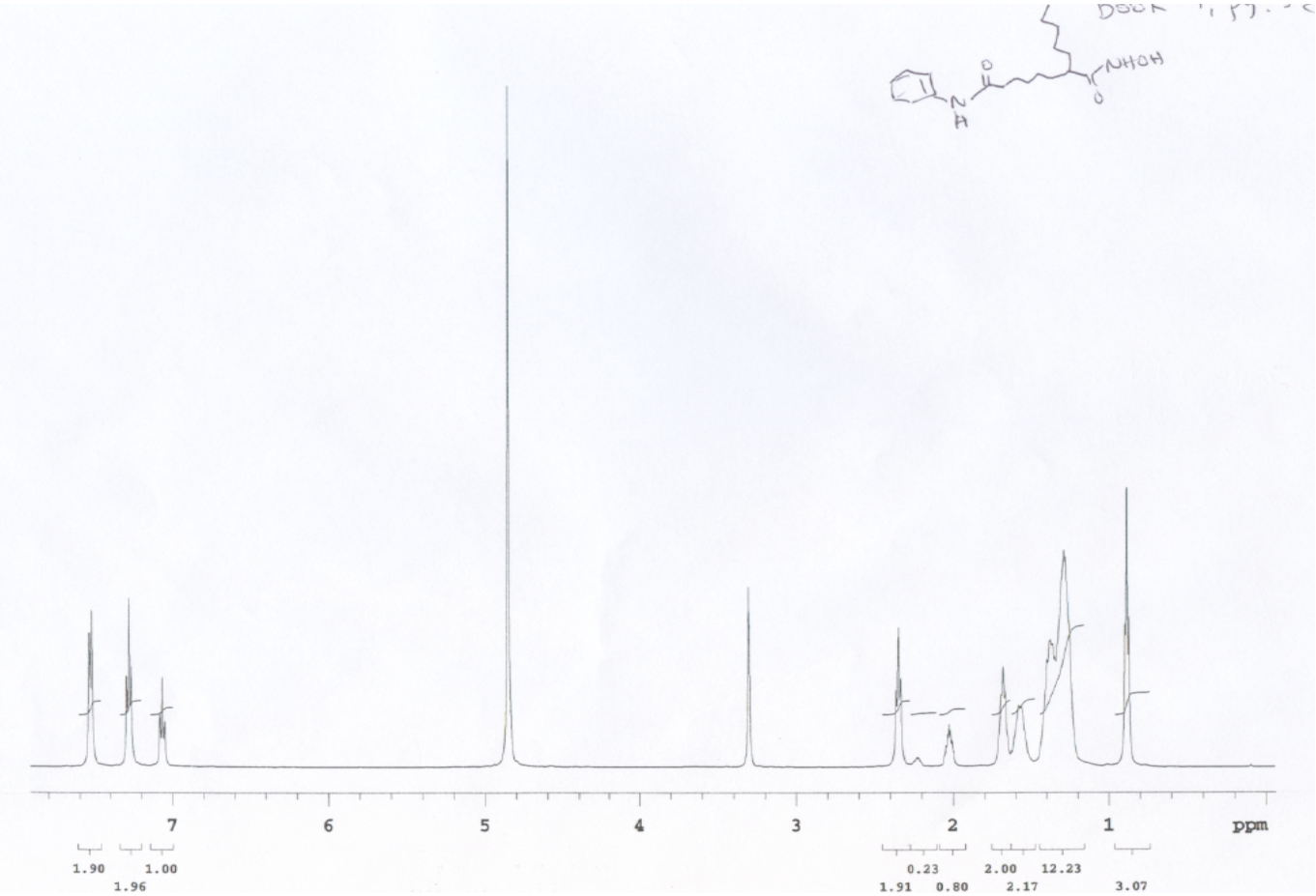

Figure S1: ^{1}H NMR spectrum of C2-*n*-pentyl SAHA (**1h**) in CD_3OD (peak at 3.3)[7] in the presence of trace amounts of water (4.8 ppm)[7] using a Varian 500 MHz instrument.

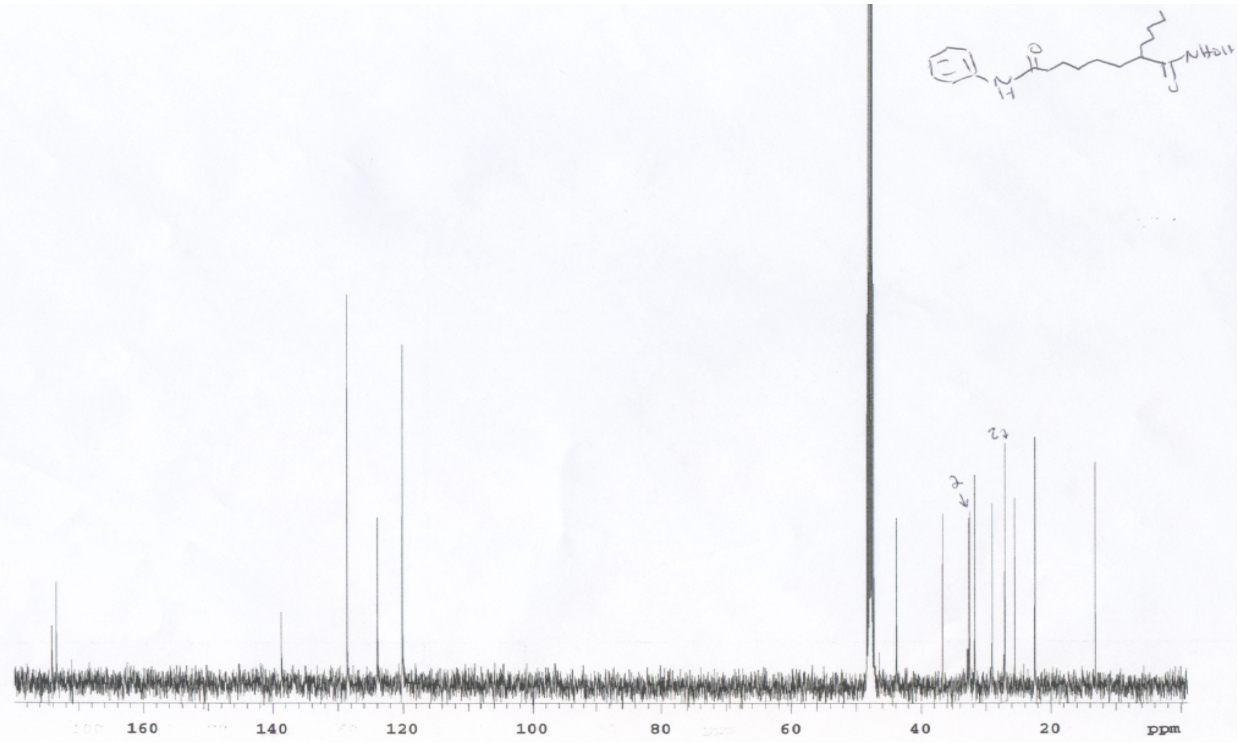

Figure S2: ^{13}C NMR spectrum of C2-*n*-pentyl SAHA (**1h**) in CD_3OD (peak at 49 ppm)[7] using a Varian 500 MHz instrument.

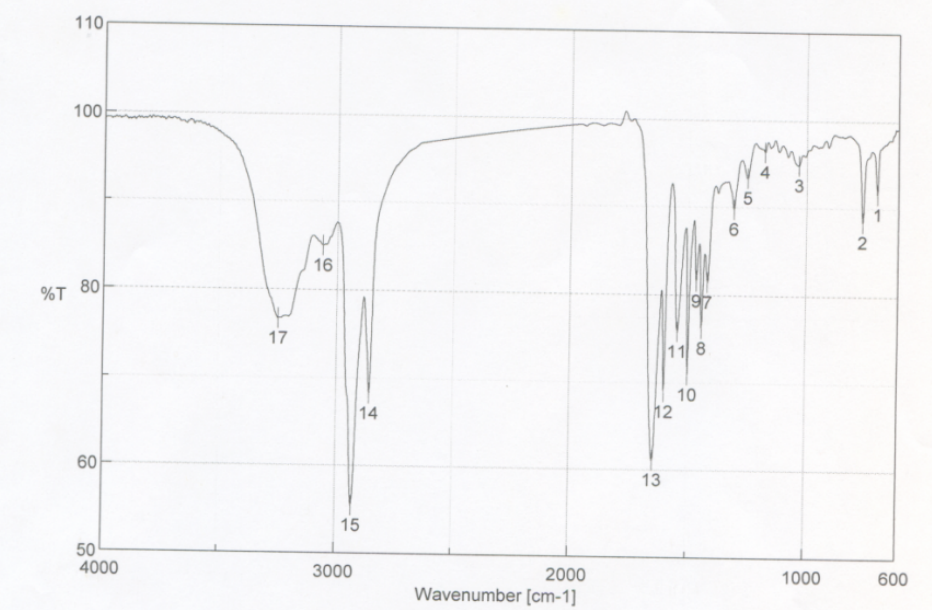

Result of Peak Picking

No.	Position	Intensity	No.	Position	Intensity
1	692.32	91.5689	2	754.995	88.3707
3	1032.69	94.7848	4	1178.29	96.2927
5	1252.54	93.2944	6	1310.39	89.7488
7	1419.35	81.3875	8	1442.49	76.1642
9	1466.6	81.5246	10	1499.38	70.8575
11	1544.7	75.8072	12	1599.66	68.8753
13	1645.95	61.0925	14	2857.02	68.1754
15	2928.38	55.4286	16	3061.44	84.9591
17	3247.54	76.6377			

[Comment]
Sample Name
Comment
User
Division
Company Wayne State

[Measurement Information]
Model Name FT/IR-4100typeA
Serial Number B071461016

Figure S3: FT/IR spectrum of C2-*n*-pentyl SAHA (**1h**) in using a Jasco FT/IR – 4100 instrument.

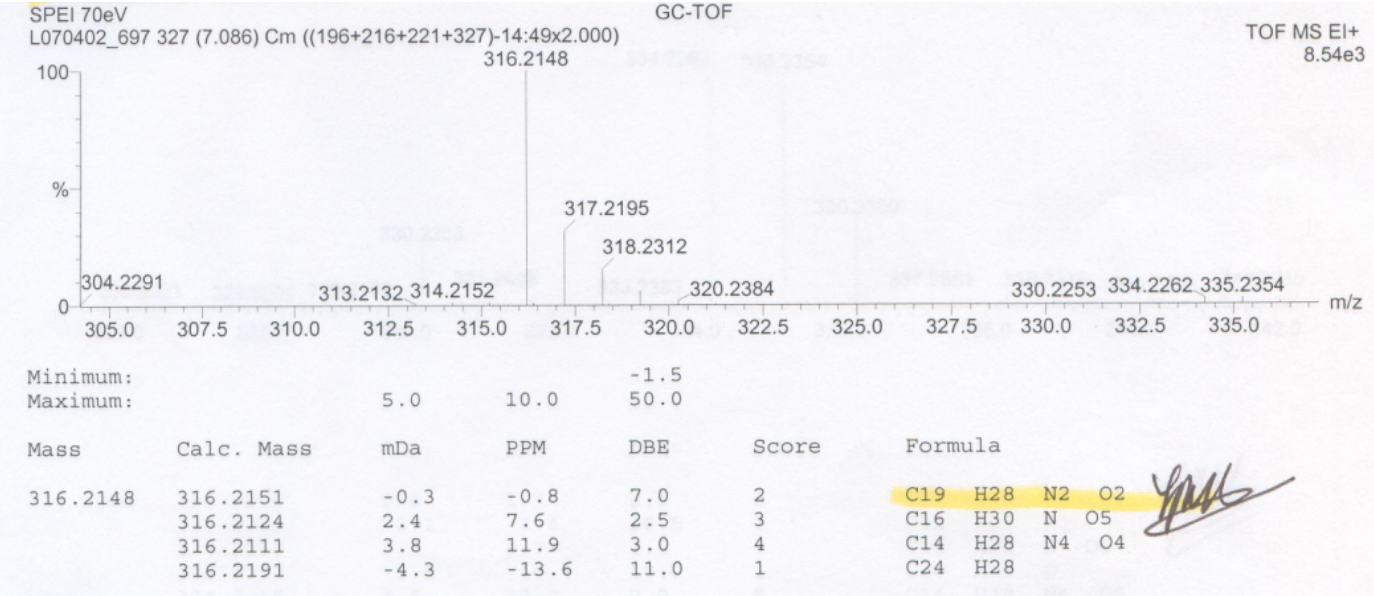

Figure S4: High resolution mass spectrum of C2-*n*-pentyl SAHA (**1h**) in using a Waters GCT EI-TOF instrument.

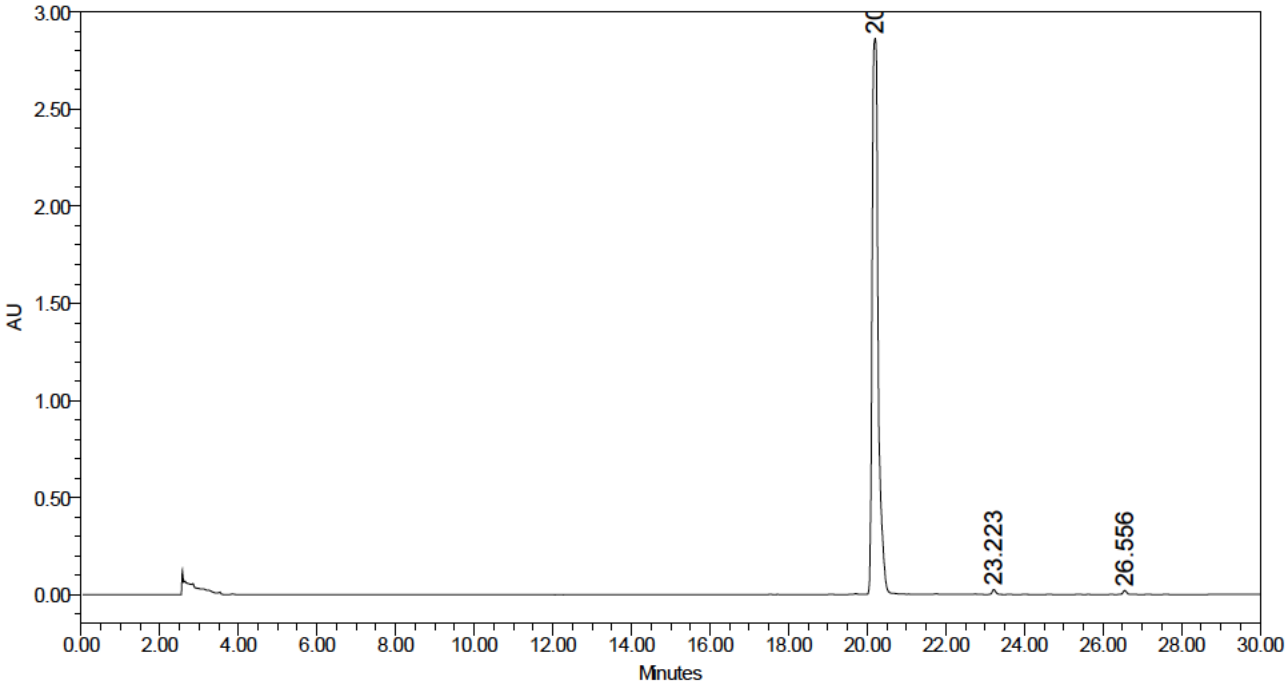

	RT	Area	% Area	Height
1	20.204	30761851	99.06	2861633
2	23.223	160202	0.52	25459
3	26.556	132825	0.43	20702

Figure S5. HPLC spectrum taken at 254 nm of C2-*n*-pentyl SAHA (**1h**). The peak at 20.2 is C2-*n*-pentyl SAHA. The calculated area and height under each peak, along with % area, is shown in the table below the spectrum.

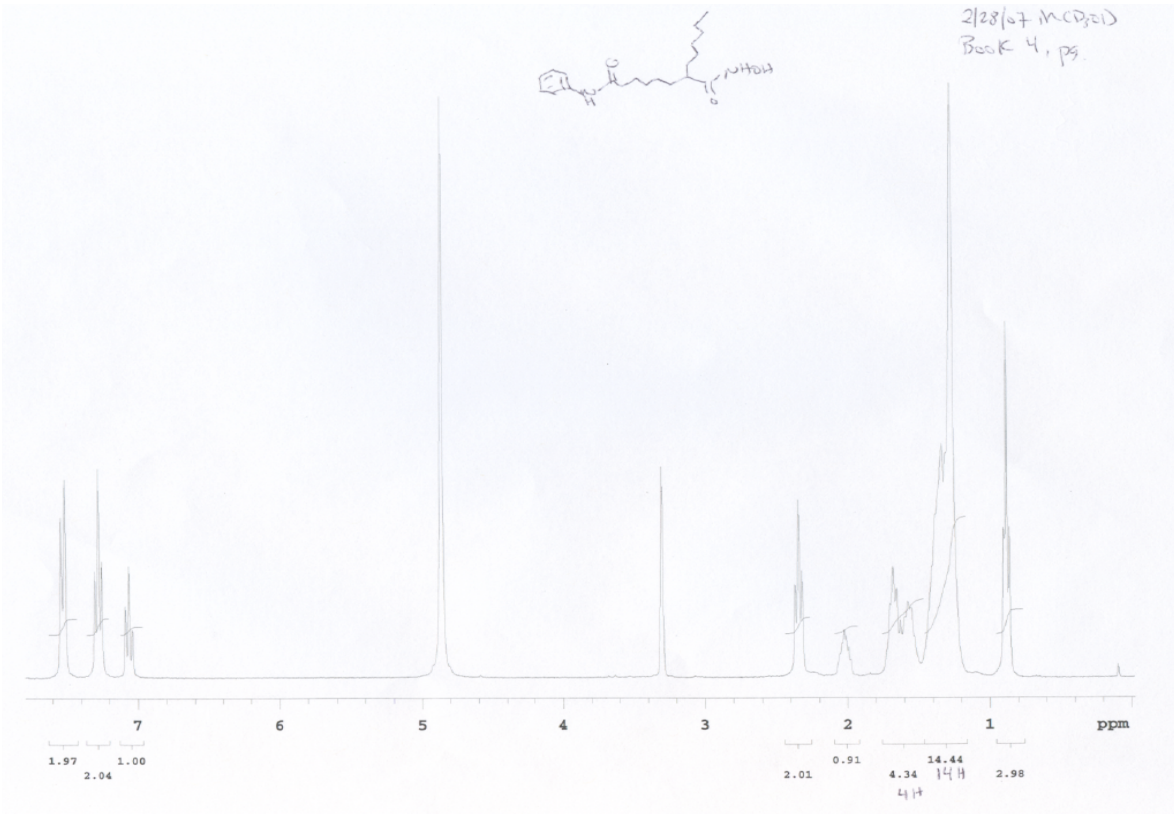

Figure S6: ^{1}H NMR spectrum of C2-*n*-hexyl SAHA (**1i**) in CD_3OD (peak at 3.3)[7] in the presence of trace amounts of water (4.8 ppm)[7] using a Varian 500 MHz instrument.

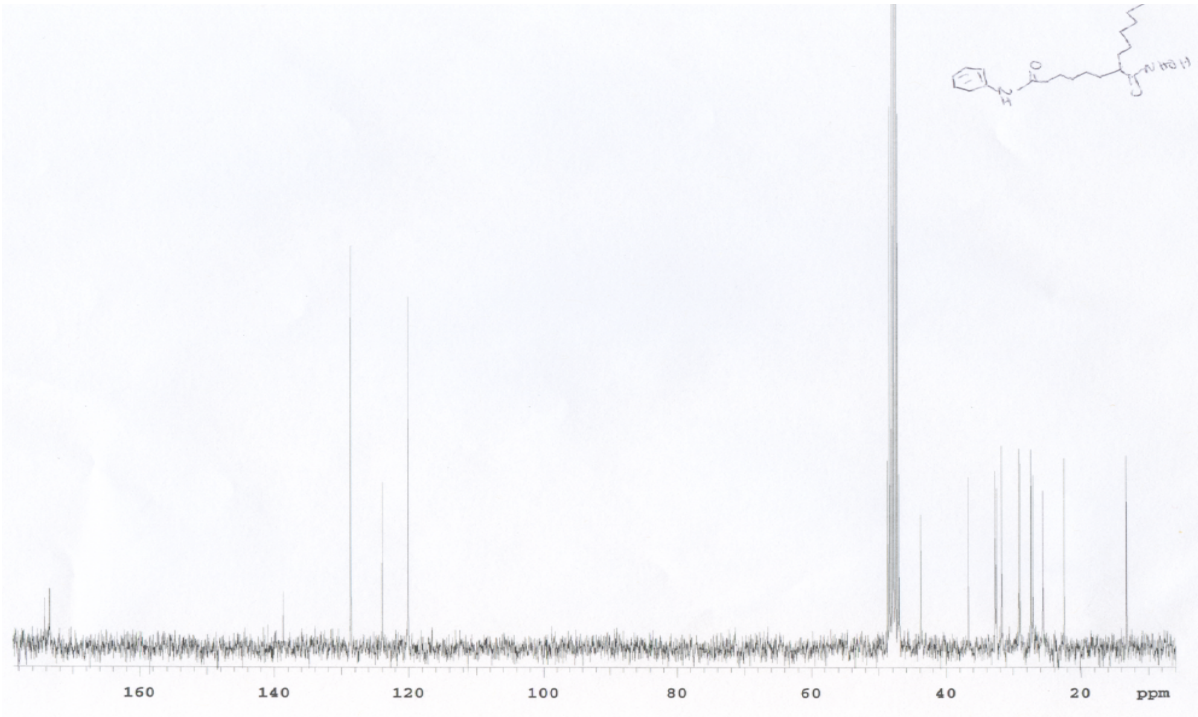

Figure S7: ^{13}C NMR spectrum of C2-*n*-hex SAHA (**1i**) in CD_3OD (peak at 49 ppm)[7] using a Varian 500 MHz instrument.

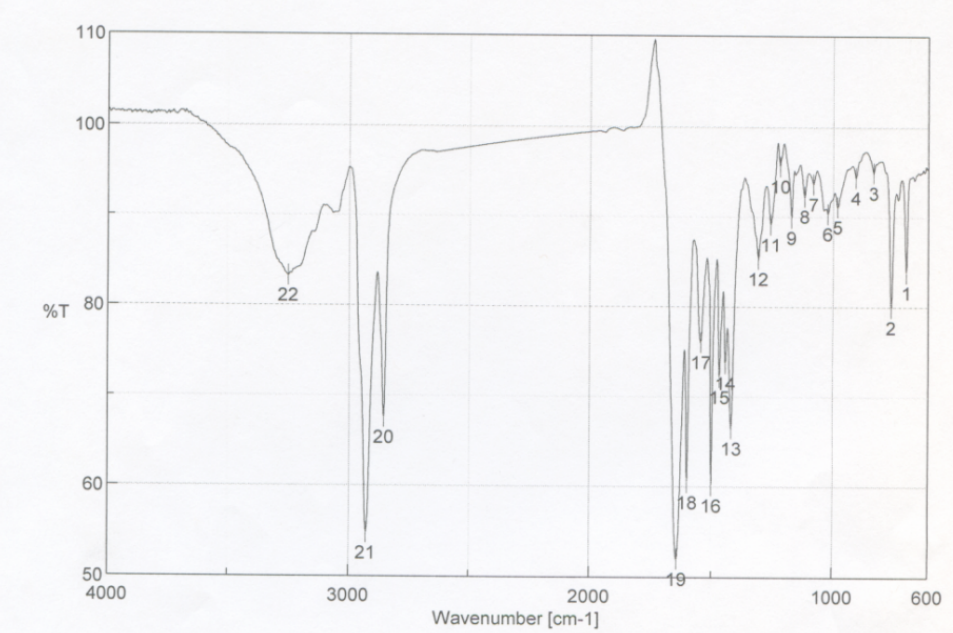

Result of Peak Picking

No.	Position	Intensity	No.	Position	Intensity
1	692.32	83.762	2	754.995	79.8877
3	830.205	94.8526	4	903.487	94.3258
5	980.625	91.0835	6	1021.12	90.3093
7	1080.91	93.6185	8	1118.51	92.2229
9	1172.51	89.8933	10	1220.72	95.5761
11	1258.32	89.0891	12	1309.43	85.2512
13	1418.39	66.3949	14	1442.49	73.6557
15	1466.6	72.1091	16	1499.38	60.1339
17	1543.74	75.9719	18	1598.7	60.448
19	1642.09	52.0144	20	2855.1	67.5121
21	2927.41	54.7828	22	3248.5	83.2545

[Comment]
Sample Name
Comment
User
Division
Company Wayne State

[Measurement Information]
Model Name FT/IR-4100typeA
Serial Number B071461016

Light Source Standard
Detector TGS

Figure S8: FT/IR spectrum of C2-*n*-hexyl SAHA (**1i**) in using a Jasco FT/IR – 4100 instrument.

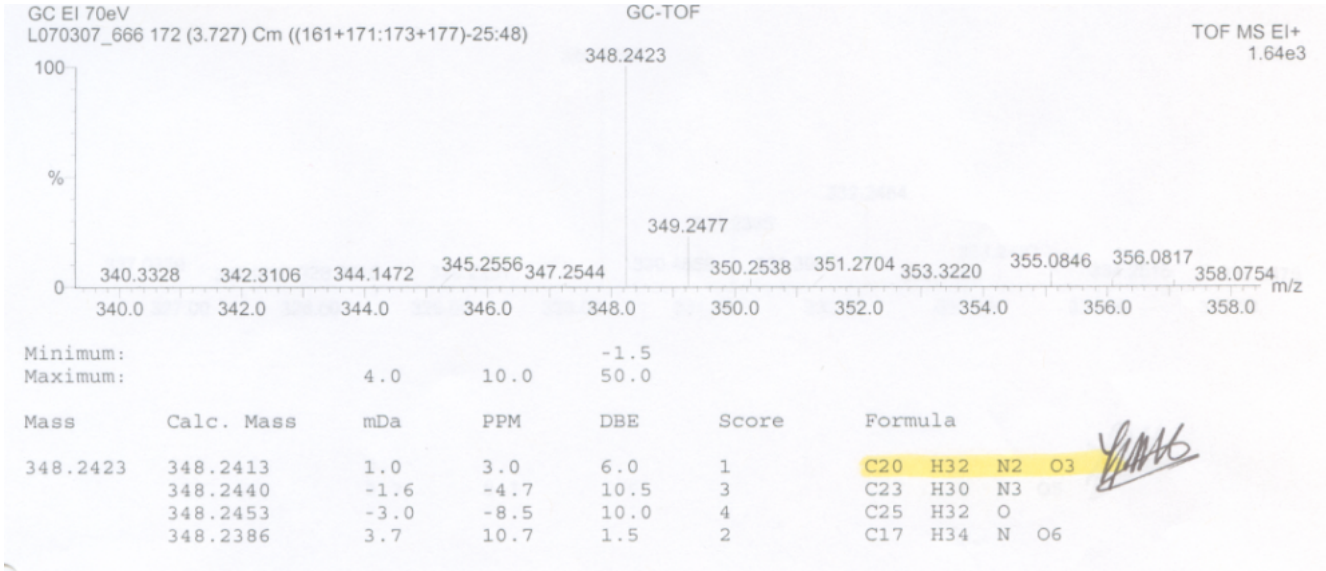

Minimum:				-1.5		
Maximum:		4.0	10.0	50.0		
Mass	Calc. Mass	mDa	PPM	DBE	Score	Formula
348.2423	348.2413	1.0	3.0	6.0	1	C20 H32 N2 O3
	348.2440	-1.6	-4.7	10.5	3	C23 H30 N3
	348.2453	-3.0	-8.5	10.0	4	C25 H32 O
	348.2386	3.7	10.7	1.5	2	C17 H34 N O6

Figure S9: High resolution mass spectrum of C2-*n*-hexyl SAHA (**1i**) in using a Waters GCT EI-TOF instrument.

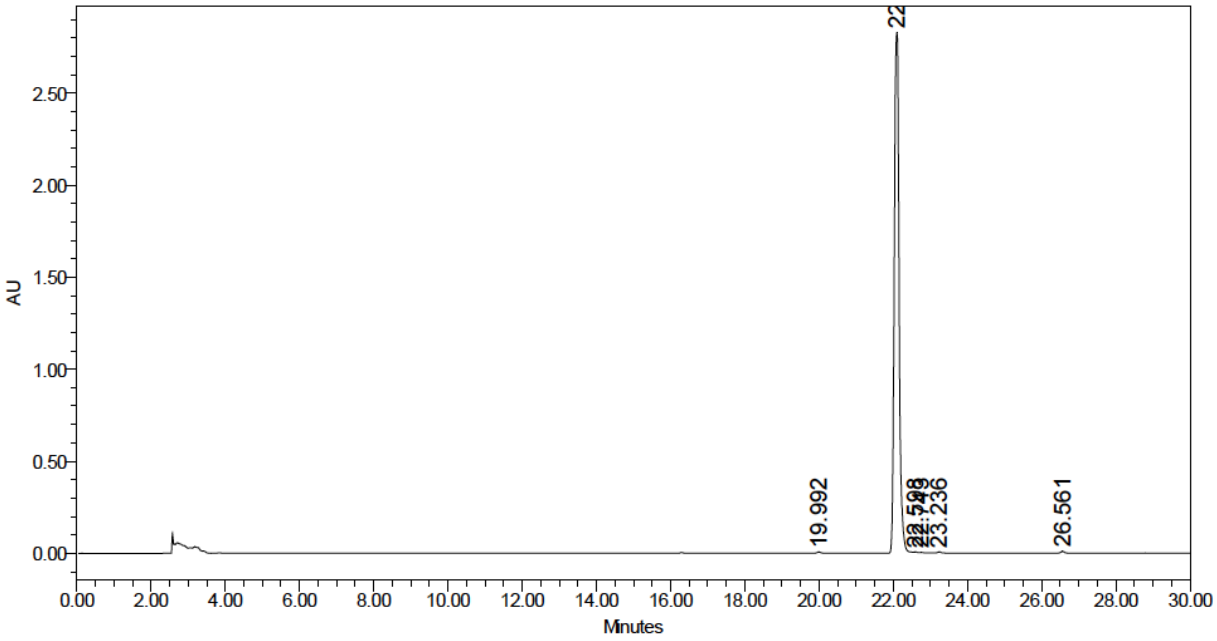

	RT	Area	% Area	Height
1	19.992	48624	0.19	6805
2	22.096	25597801	99.04	2828223
3	22.598	46775	0.18	6014
4	22.743	38957	0.15	3814
5	23.236	45360	0.18	6604
6	26.561	68019	0.26	9841

Figure S10. HPLC spectrum taken at 254 nm of C2-*n*-hexyl SAHA (**1i**). The peak at 22.1 is C2-*n*-hexyl SAHA. The calculated area and height under each peak, along with % area, is shown in the table below the spectrum.

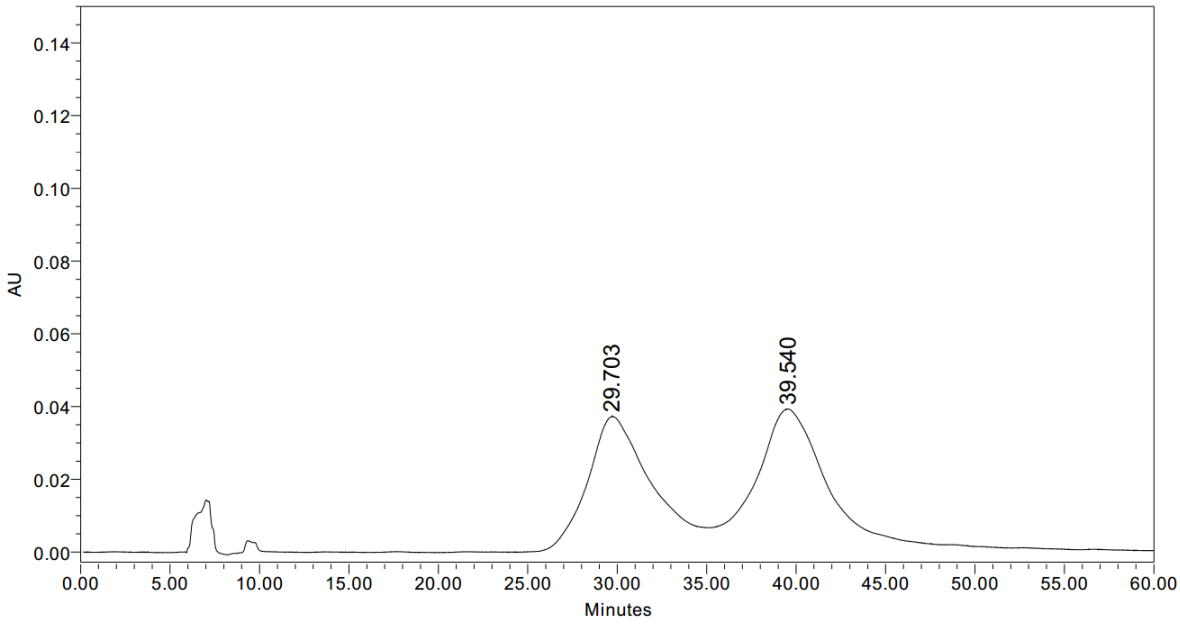

	RT	Area	% Area	Height
1	29.703	8936939	48.38	36430
2	39.540	9535849	51.62	37171

Figure S11. Chiral HPLC spectrum of the C2-*n*-hexyl SAHA (**1i**) as a racemic mixture taken at 254 nm. The spectrum shows peaks for both the *R* and the *S* enantiomers. The calculated area and height under each peak, along with % area, is shown in the table below the spectrum.

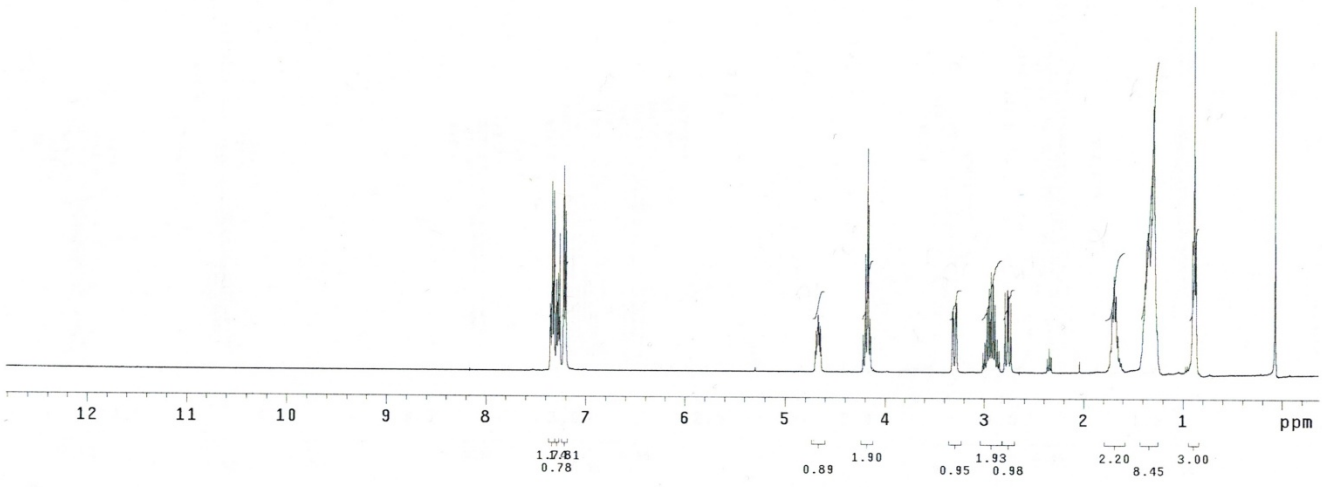

Figure S12: ^{1}H NMR spectrum of **(S)-9**.

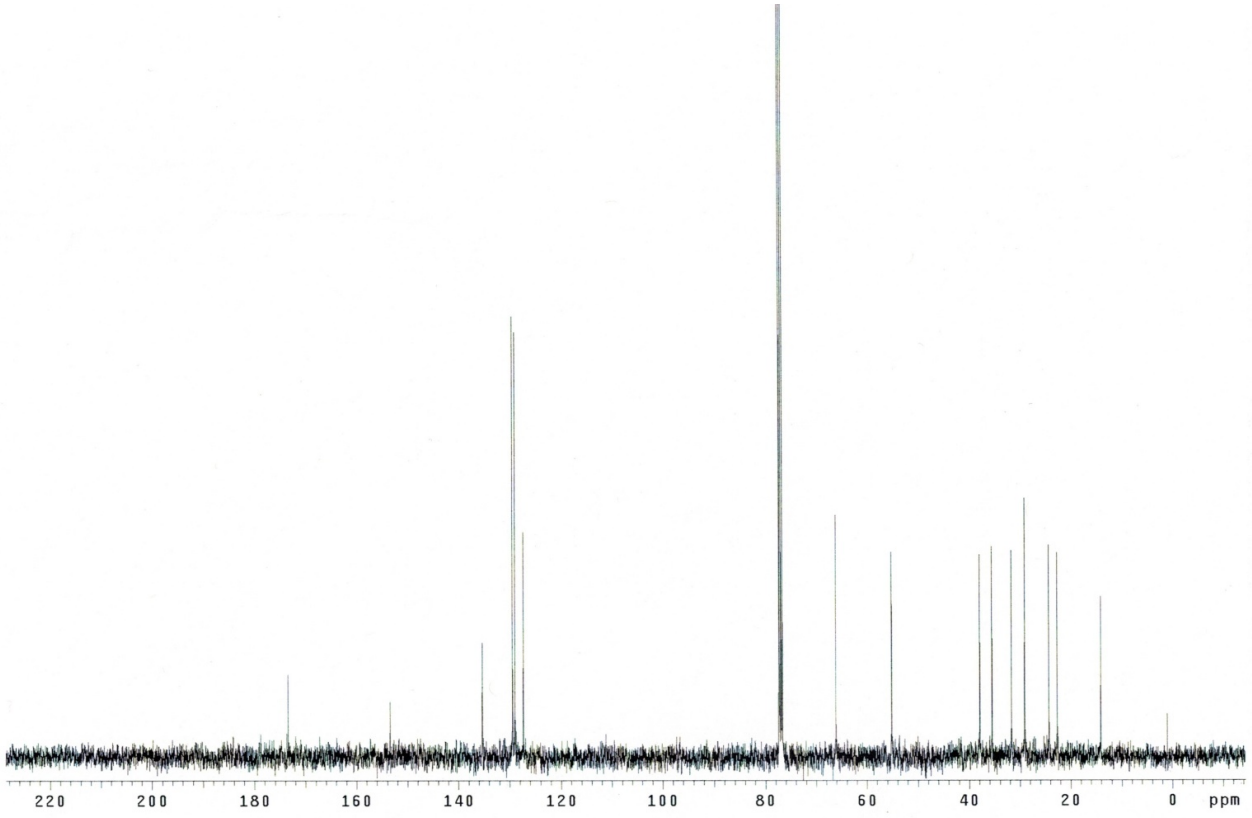

Figure S13: ^{13}C NMR spectrum of **(S)-9**.

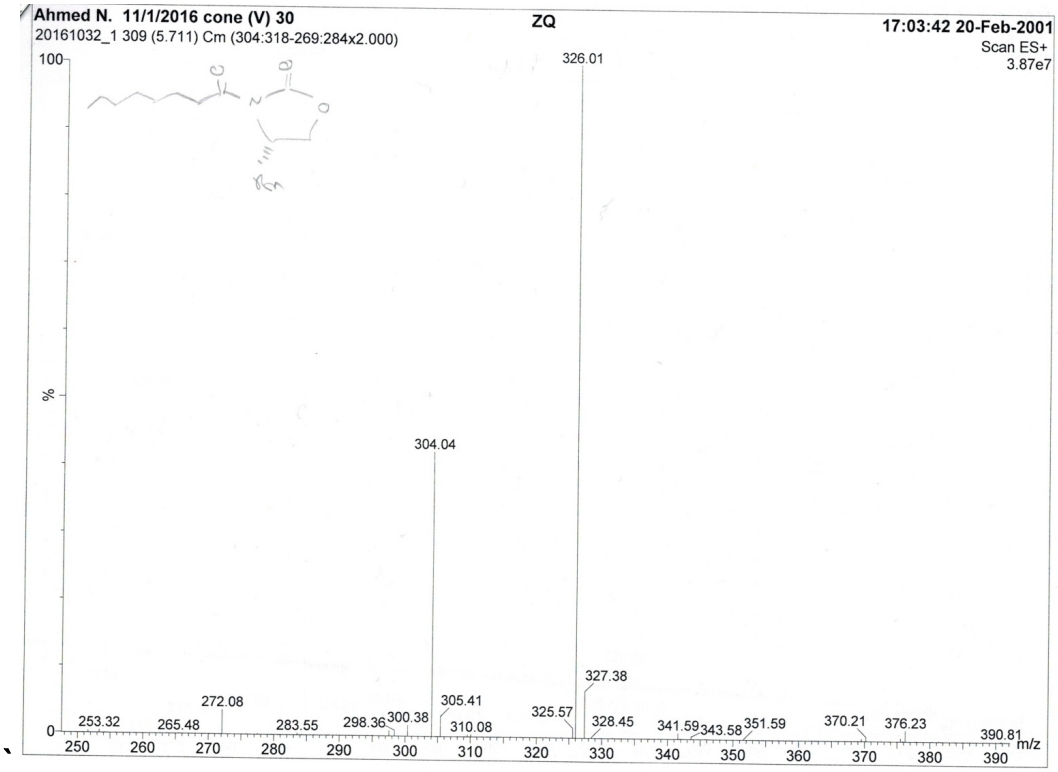

Figure S14: Low resolution mass spectrum of **(S)-9**.

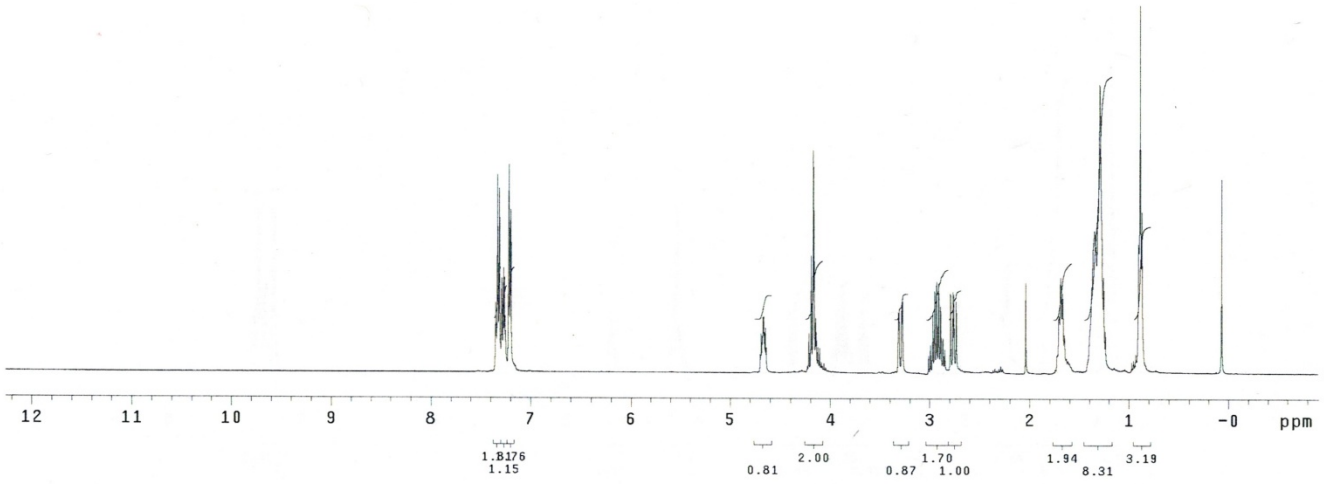

Figure S15: ^{1}H NMR spectrum of **(R)-9**.

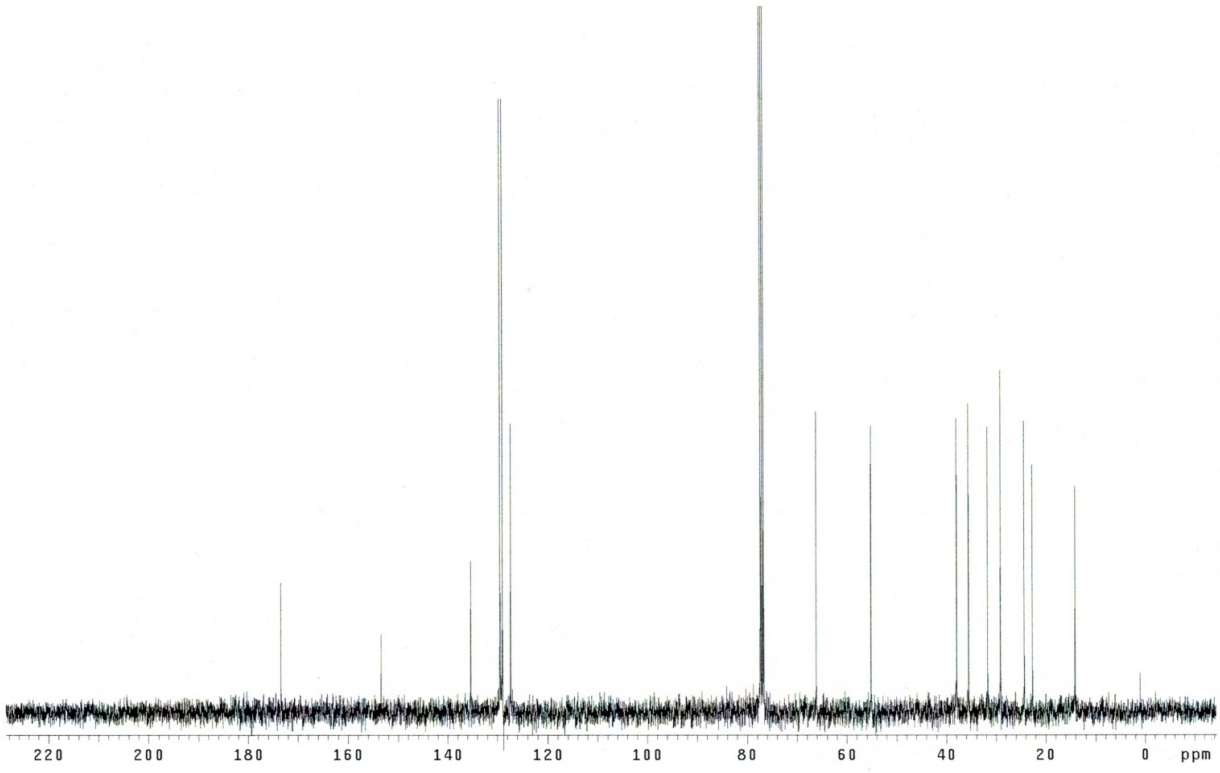

Figure S16: ^{13}C NMR spectrum of **(R)-9**.

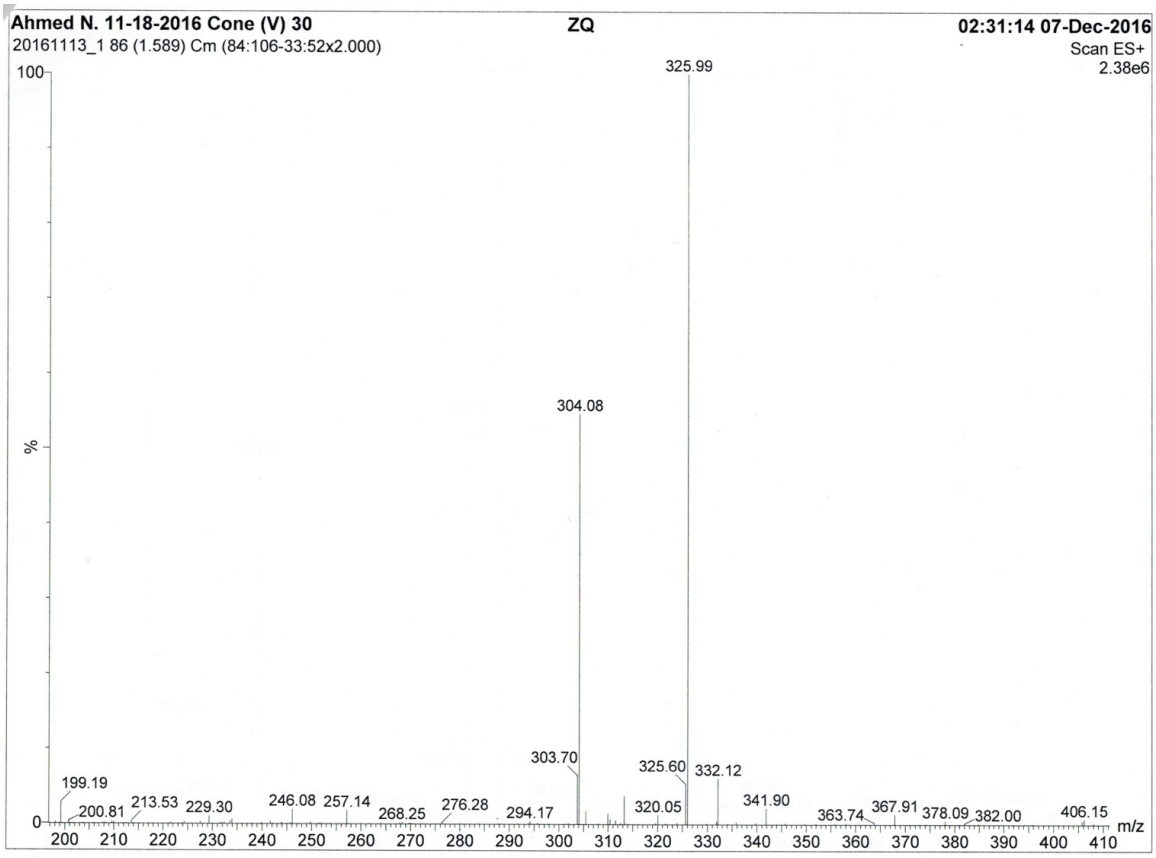

Figure S17: Low resolution mass spectrum of **(R)-9**.

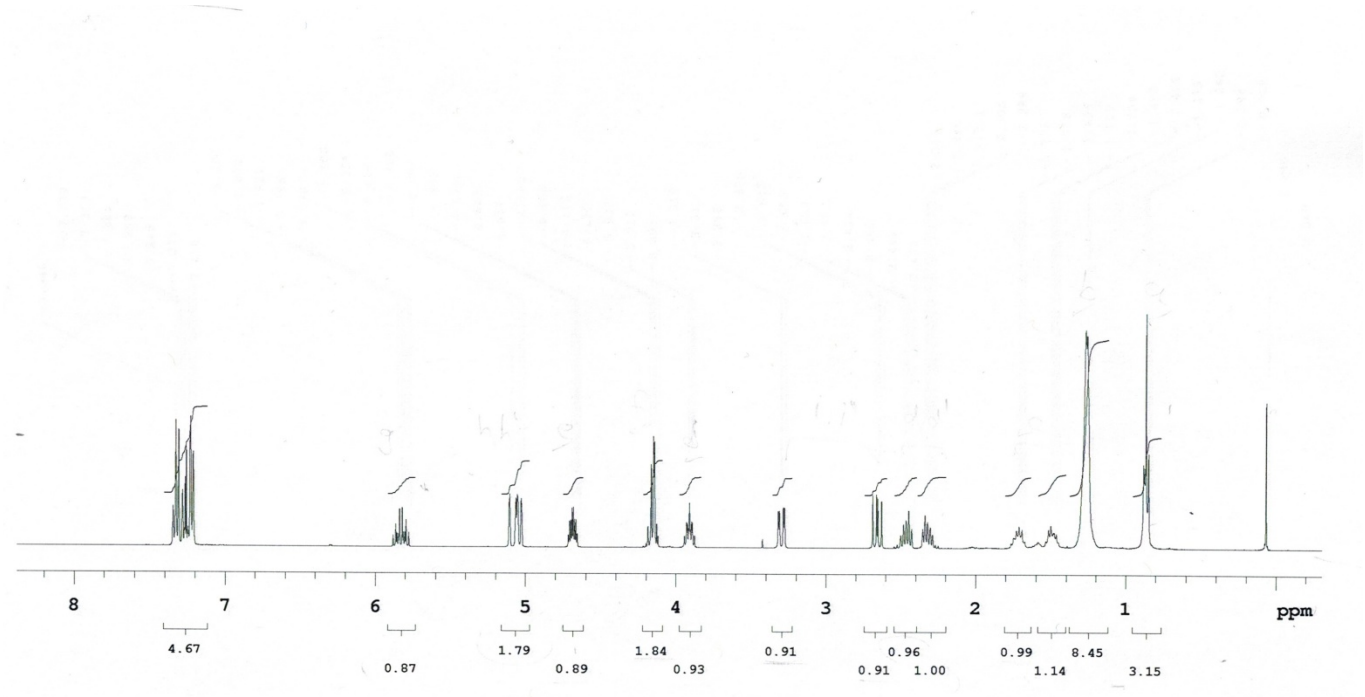

Figure S18: ^{1}H NMR spectrum of **(S)-10**.

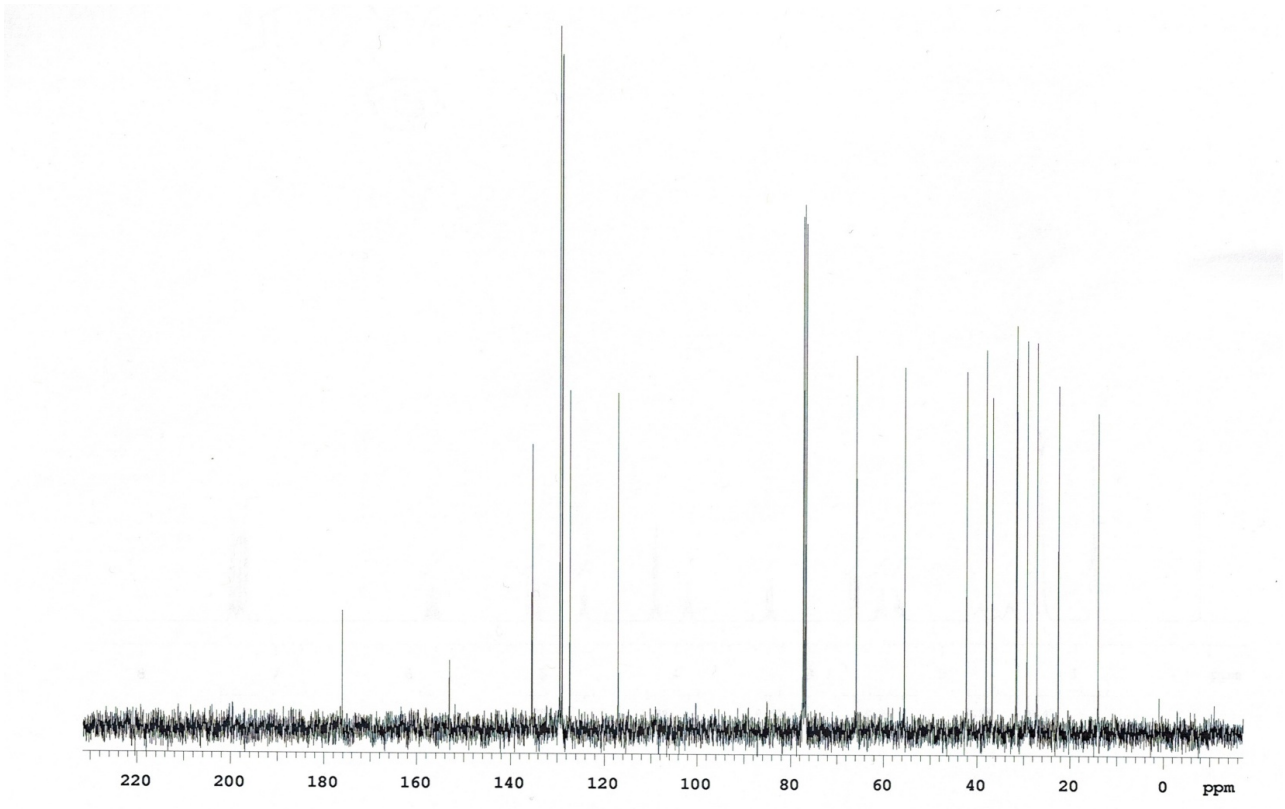

Figure S19: ^{13}C NMR spectrum of **(S)-10**.

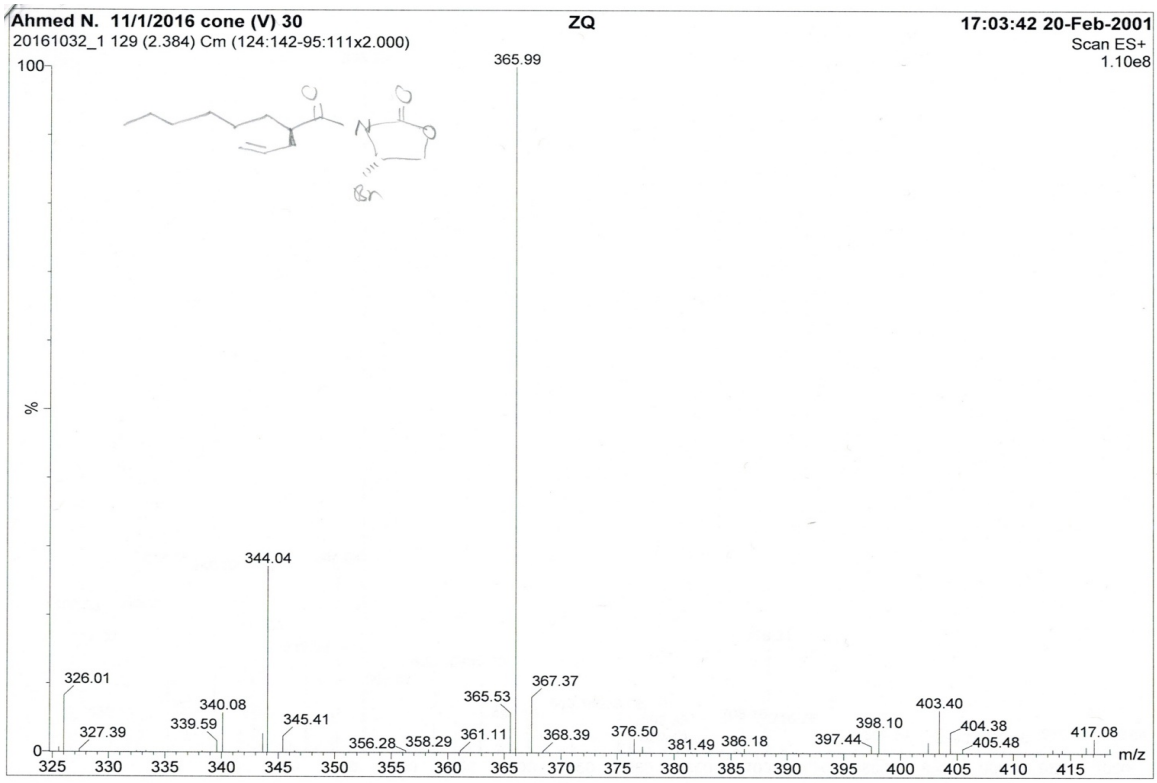

Figure S20: Low resolution mass spectrum of **(S)-10**.

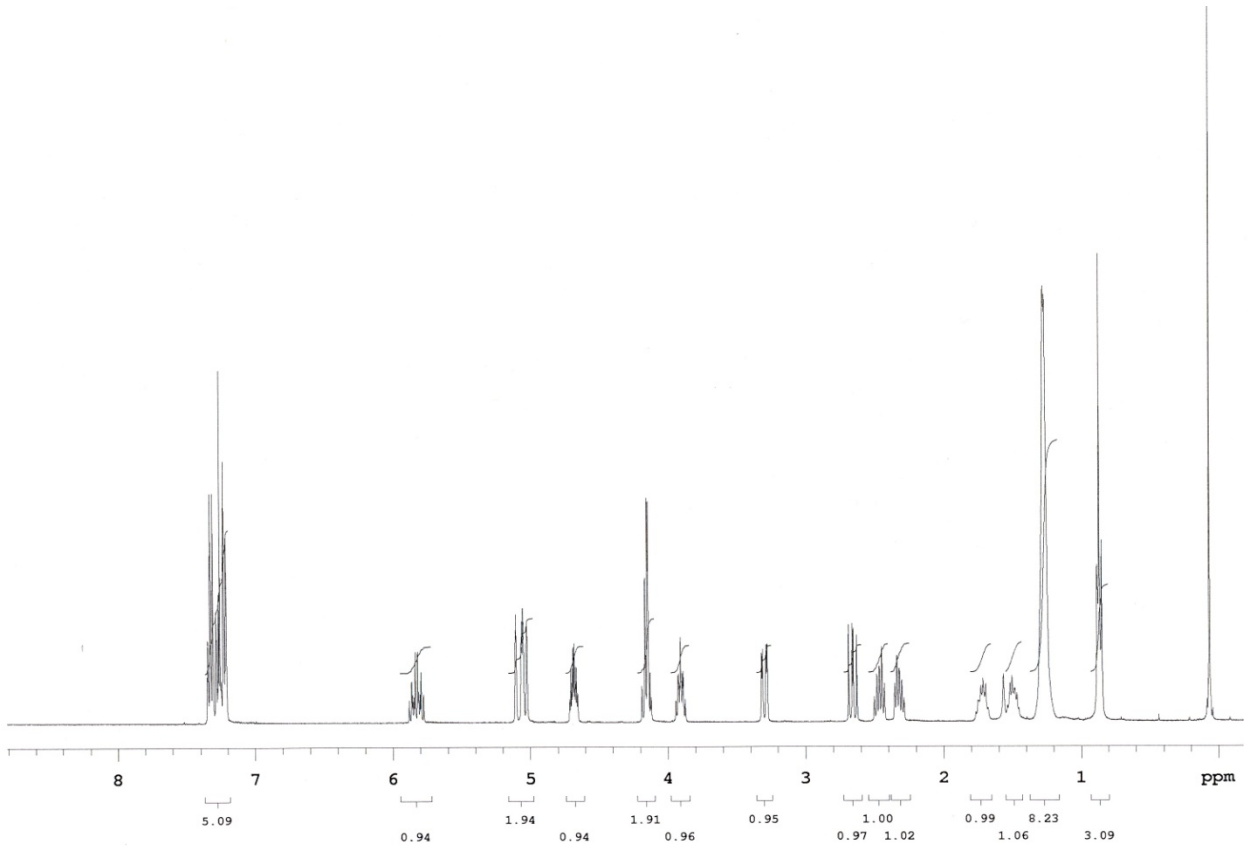

Figure S21: ^{1}H NMR spectrum of **(R)-10**.

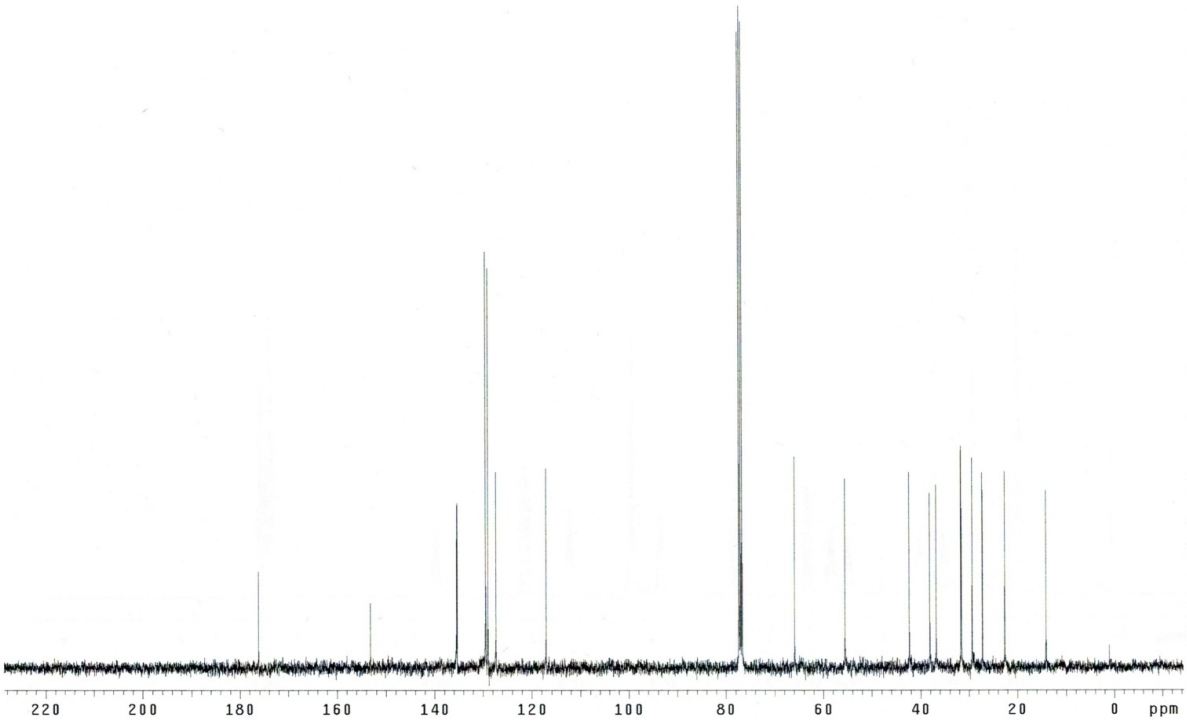

Figure S22: ^{13}C NMR spectrum of **(R)-10**.

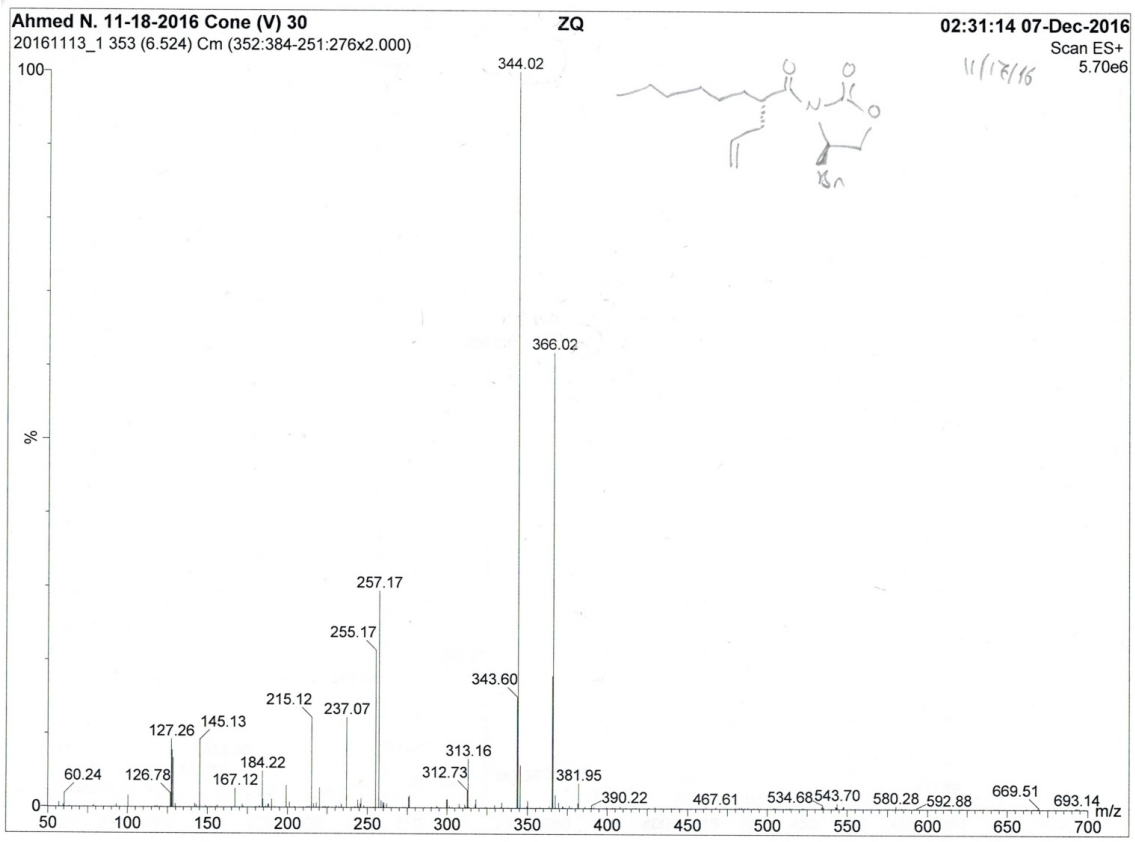

Figure S23: Low resolution mass spectrum of **(R)-10**.

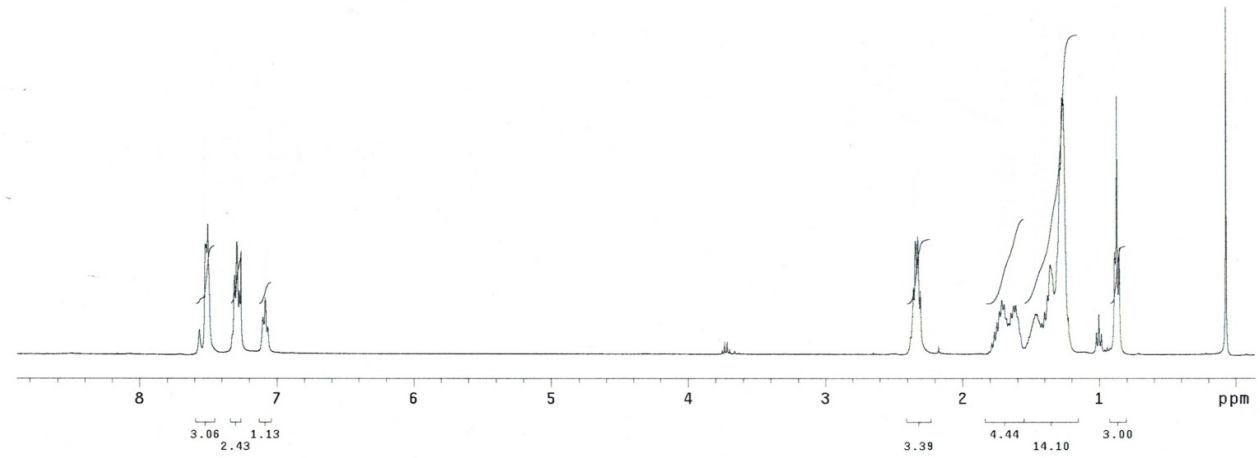

Figure S24: ^{1}H NMR spectrum of **(R)-11**.

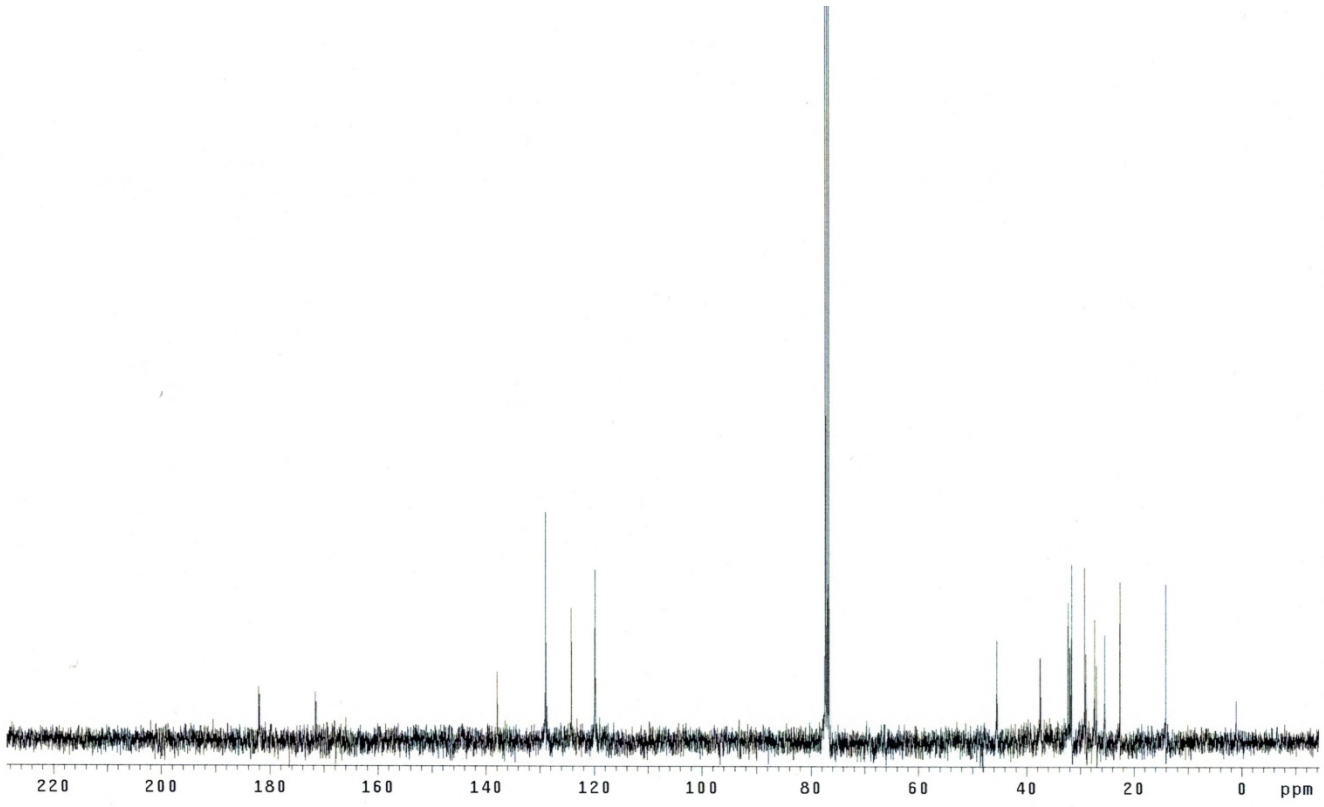

Figure S25: ^{13}C NMR spectrum of **(R)-11**.

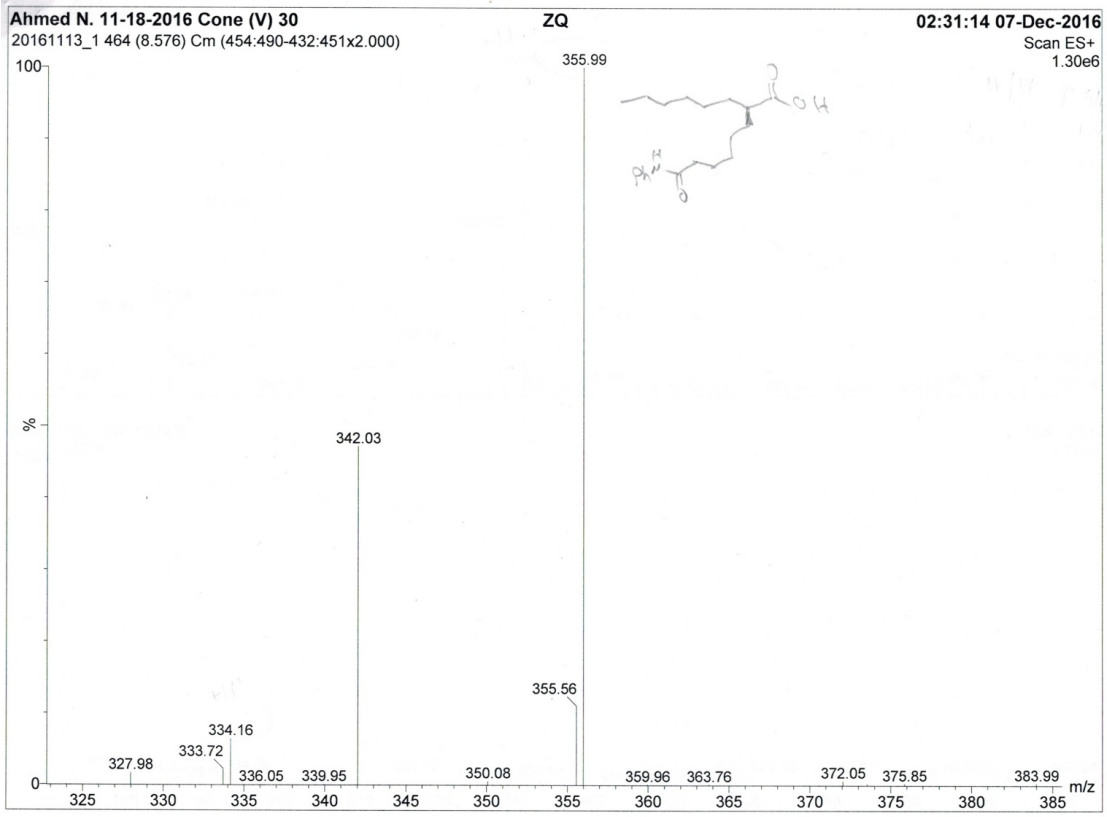

Figure S26: Low resolution mass spectrum of **(R)-11**.

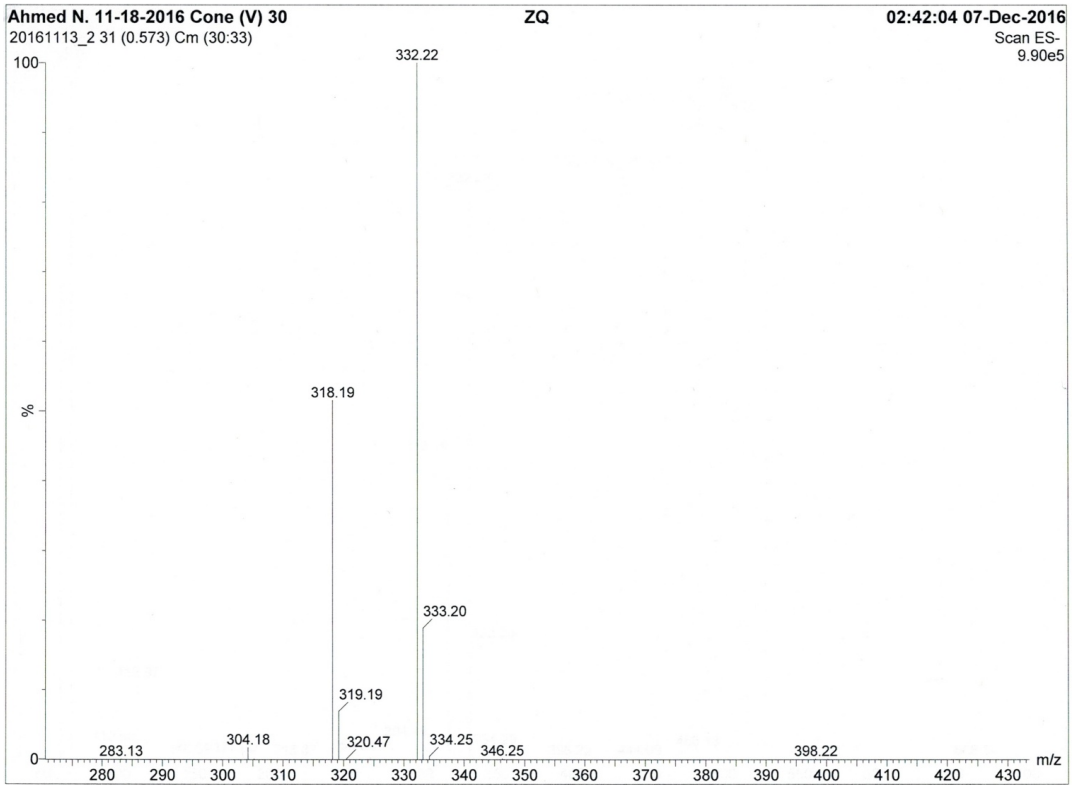

Figure S27: Low resolution mass spectrum of **(R)-11**.

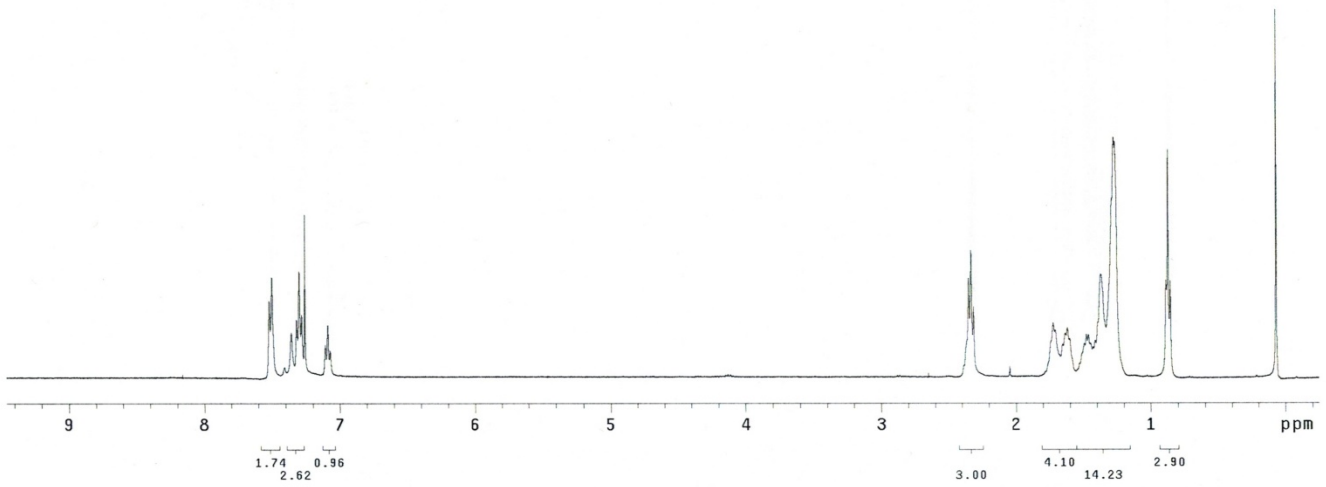

Figure S28: ^{1}H NMR spectrum of **(S)-11**.

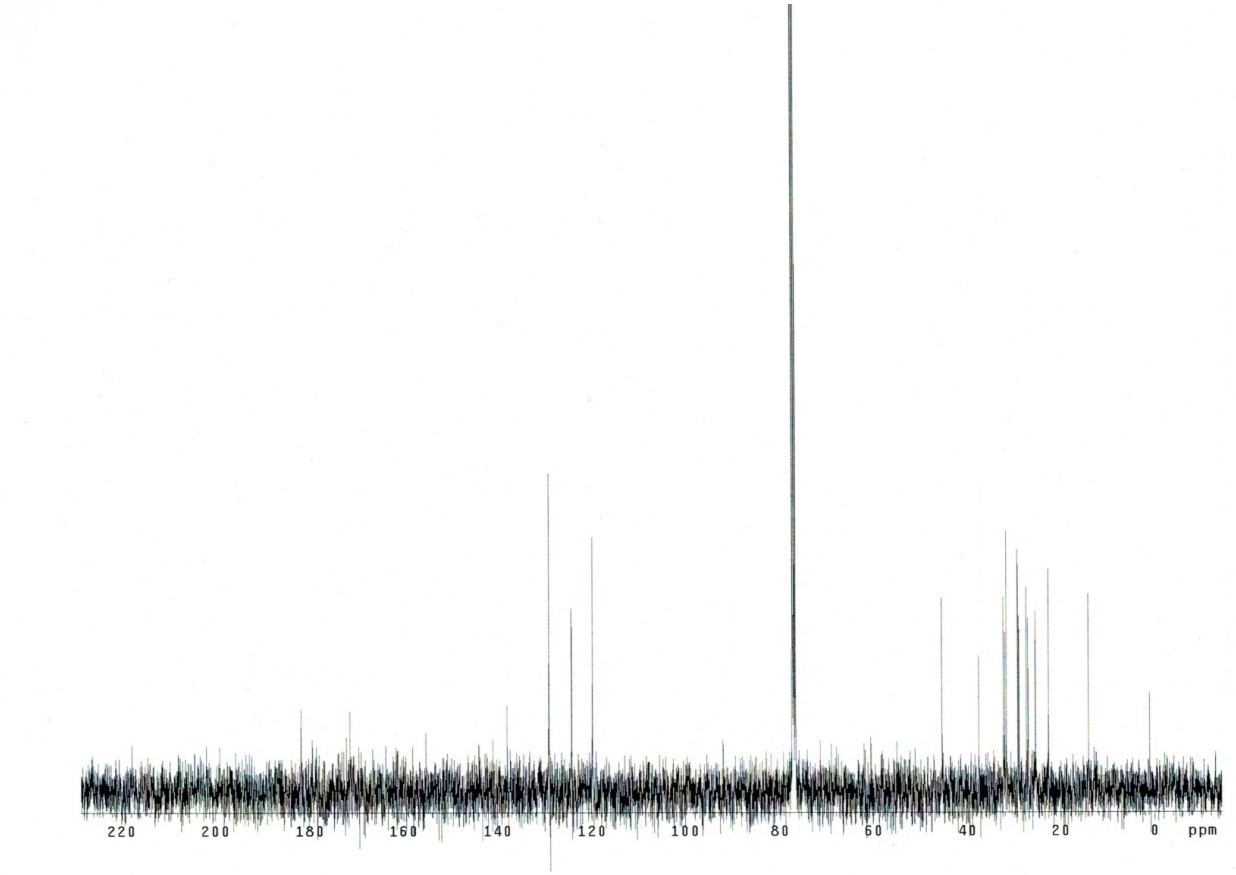

Figure S29: ^{13}C NMR spectrum of **(S)-11**.

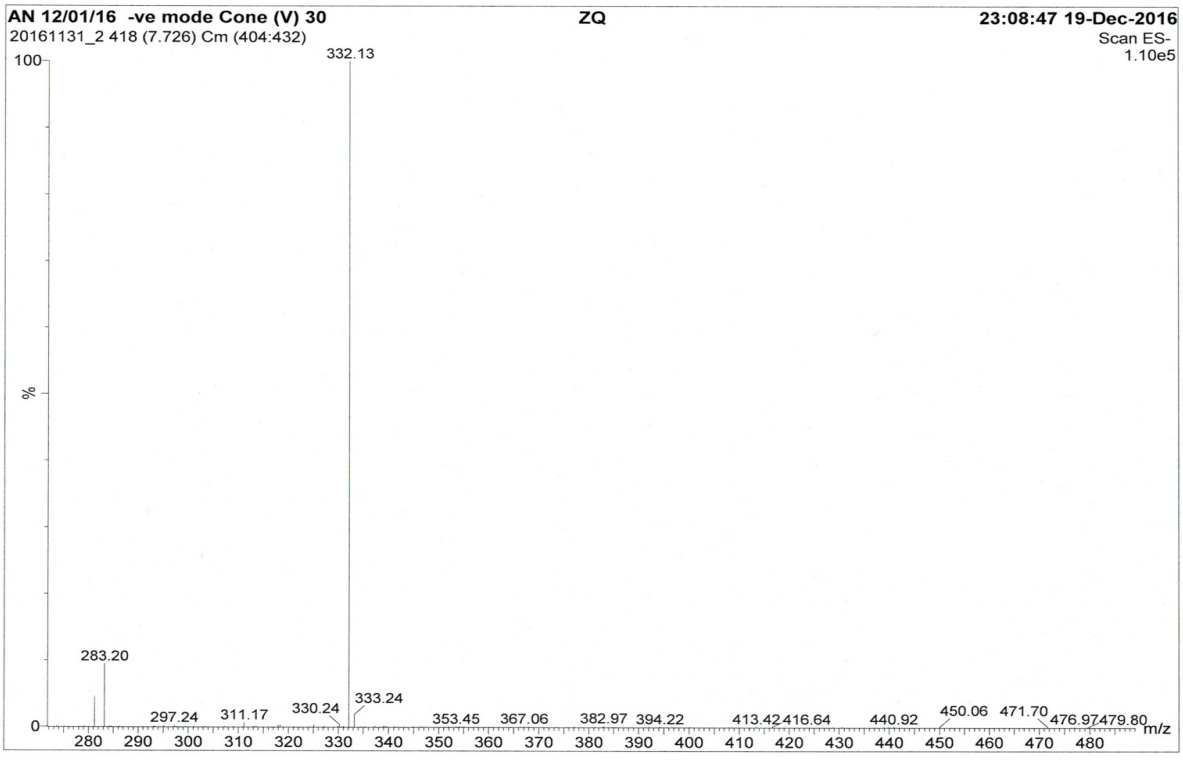

Figure S30: Low resolution mass spectrum of **(S)-11**.

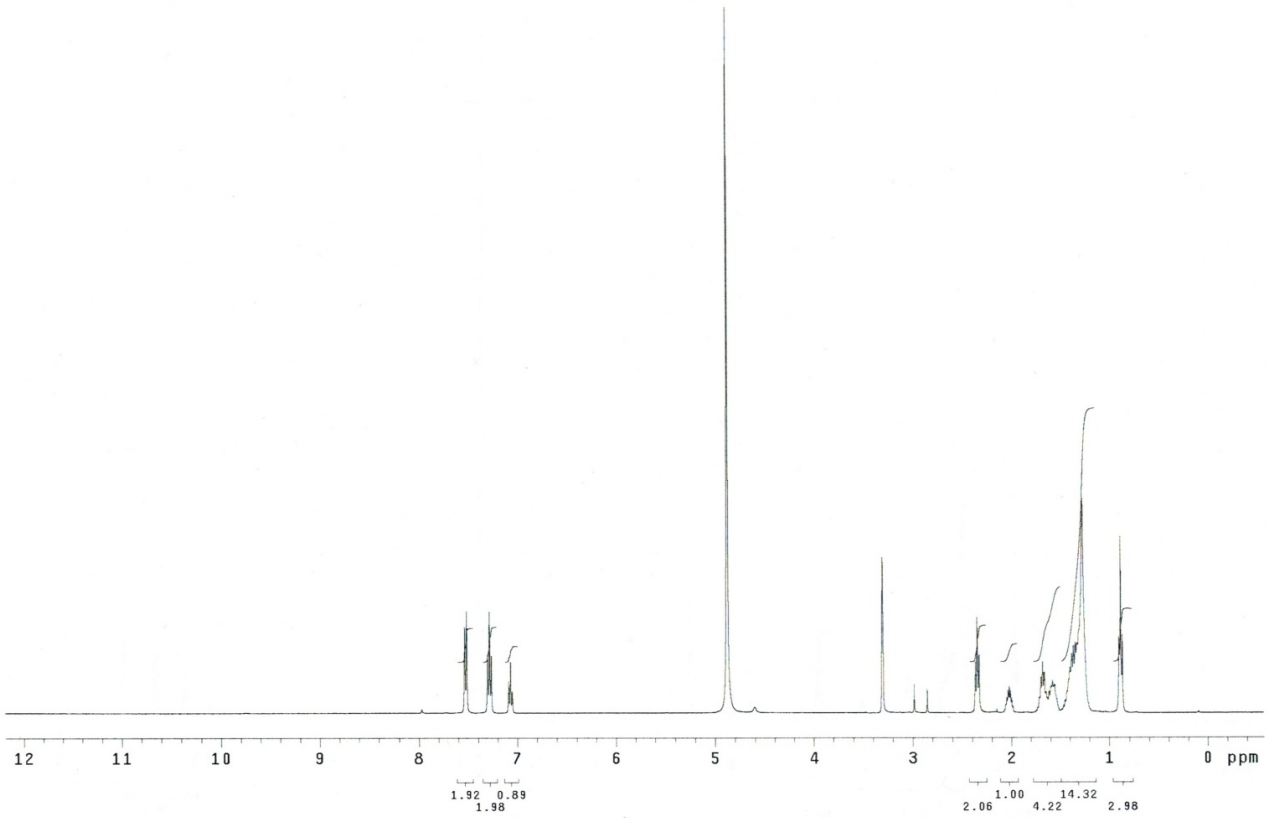

Figure S31: ^{1}H NMR spectrum of R-C2-*n*-hexyl SAHA (**R-1i**).

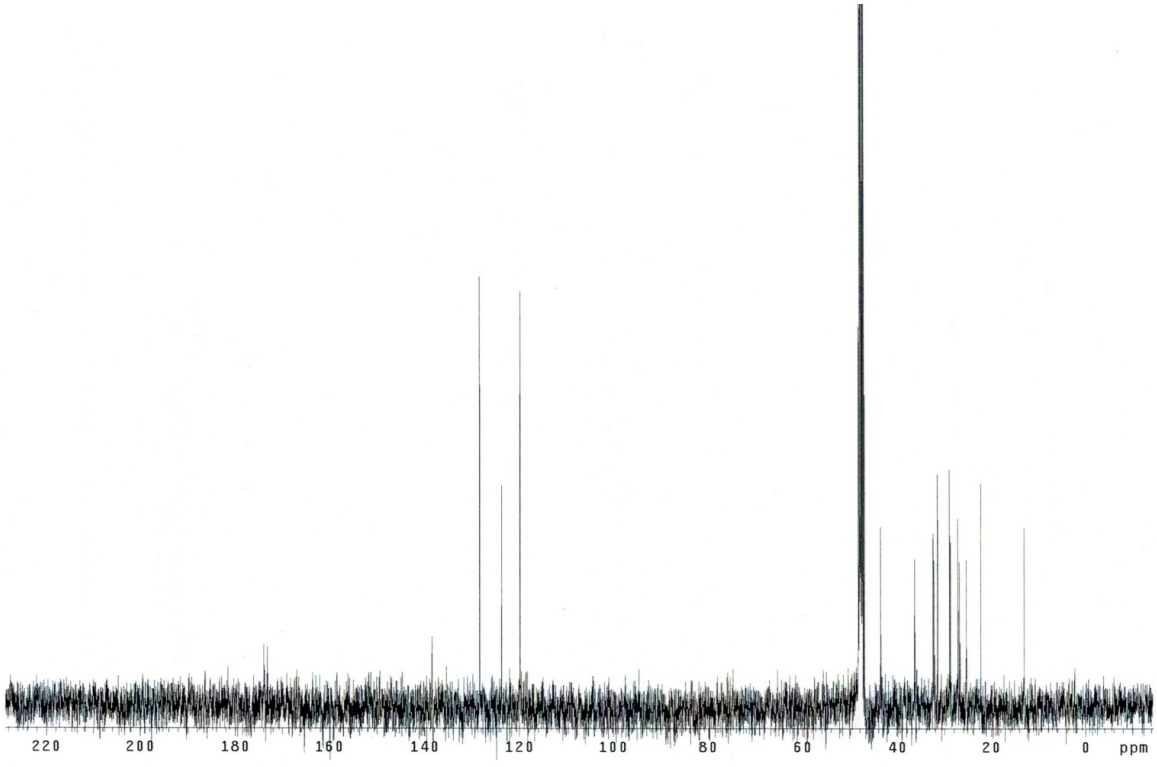

Figure S32: ^{13}C NMR spectrum of R-C2-*n*-hexyl SAHA (**R-1i**)

Elemental Composition Report **Page 1**

Single Mass Analysis
Tolerance = 20.0 PPM / DBE: min = -1.5, max = 100.0
Element prediction: Off
Number of isotope peaks used for i-FIT = 6

Monoisotopic Mass, Even Electron Ions
619 formula(e) evaluated with 1 results within limits (all results (up to 1000) for each mass)
Elements Used:
C: 20-20 H: 0-50 N: 0-50 O: 0-50 Na: 0-1

AhmadN R_C2hexyl 12-08-2016 (V) 50

LCT Premier KD128
TOF MS ES+

3.41e+005

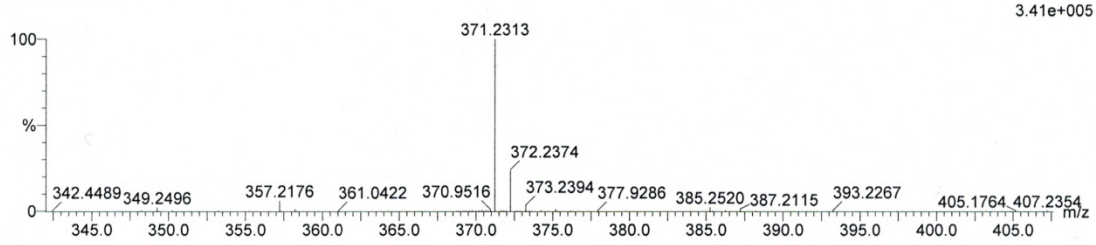

Minimum:				-1.5			
Maximum:		3.0	20.0	100.0			
Mass	Calc. Mass	mDa	PPM	DBE	i-FIT	i-FIT (Norm)	Formula
371.2313	371.2311	0.2	0.5	5.5	160.9	0.0	C20 H32 N2 O3 Na

Figure S33: High resolution mass spectrum of (R)-C2-*n*-hexyl SAHA (R-**1i**).

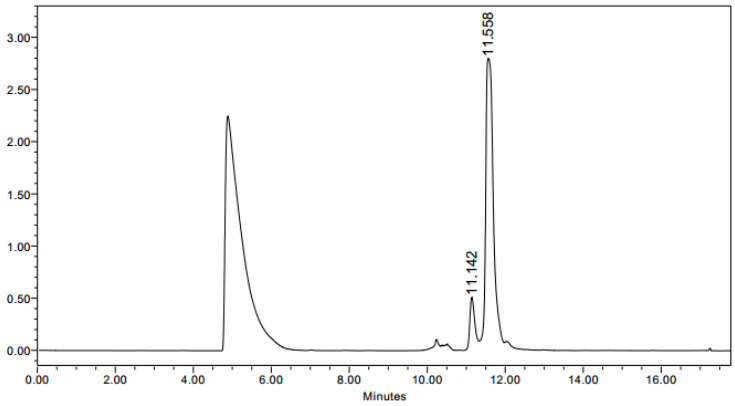

	RT	Area	% Area	Height
1	11.142	4496704	10.54	497410
2	11.558	38171650	89.46	2786557

Figure S34. HPLC spectrum taken at 254 nm of R-C2-*n*-hexyl SAHA (**R-1h**). The calculated area and height under each peak, along with % area, is shown in the table below the spectrum.

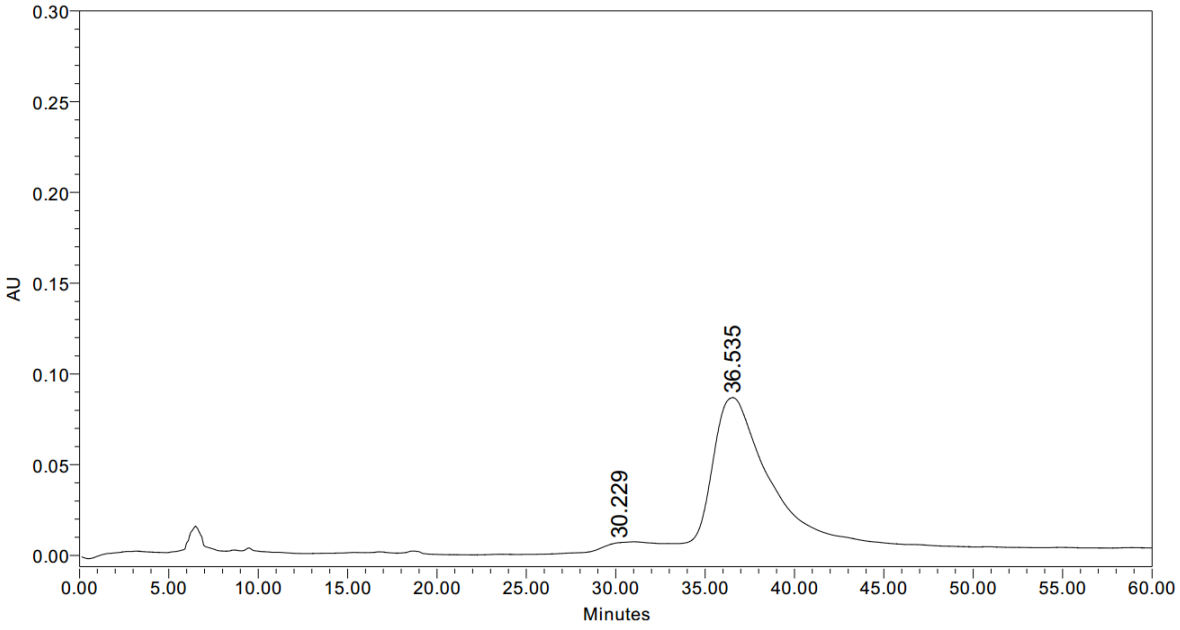

	RT	Area	% Area	Height
1	30.229	627338	3.97	3519
2	36.535	15190243	96.03	78984

Figure S35. Chiral HPLC spectrum of the (*R*)-C2-*n*-hexyl SAHA (**R-1i**) taken at 254 nm. The major peak (36.5 min) represents the *R* enantiomer, while the minor peak (30.2 min) represents the *S* enantiomer (see Figure S11). The calculated area and height under each peak, along with % area, is shown in the table below the spectrum.

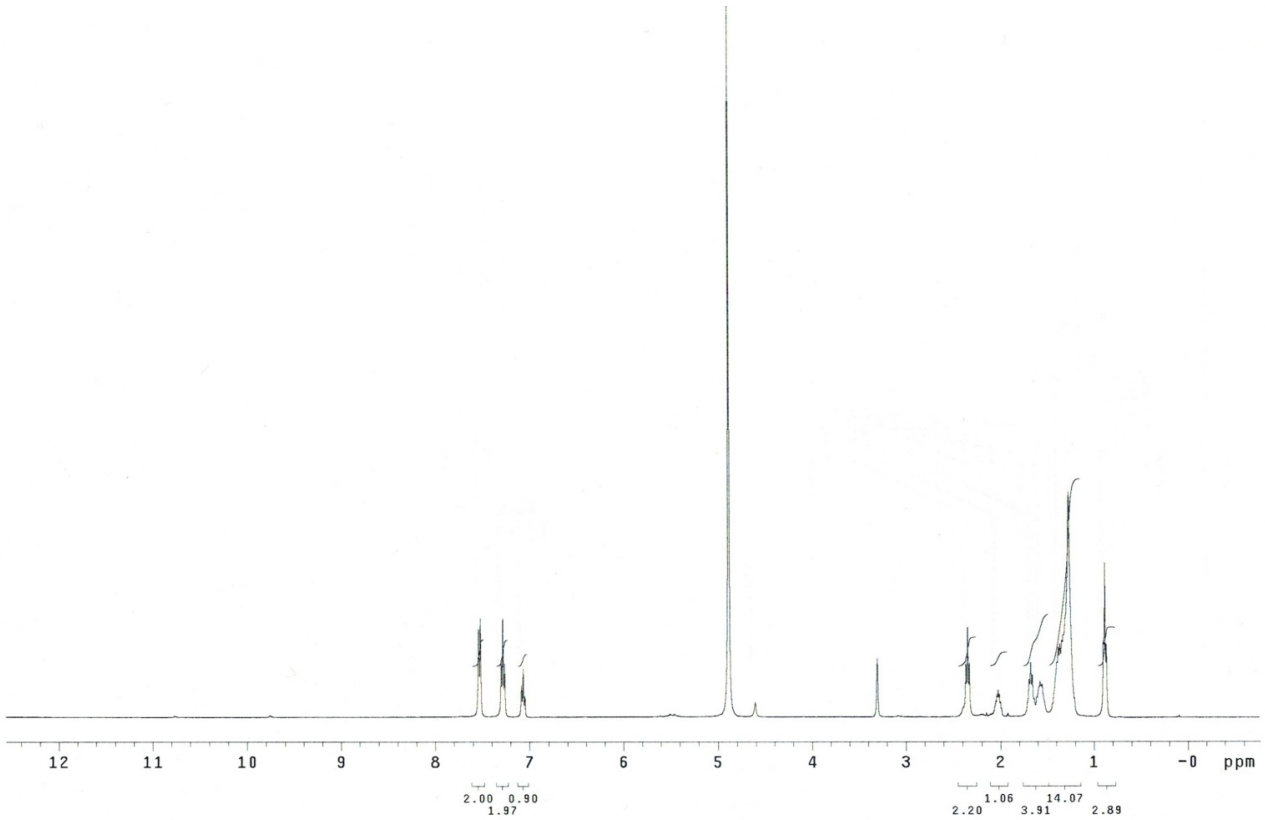

Figure S36: ^{1}H NMR spectrum of S-C2-*n*-hexyl SAHA (**S-1i**).

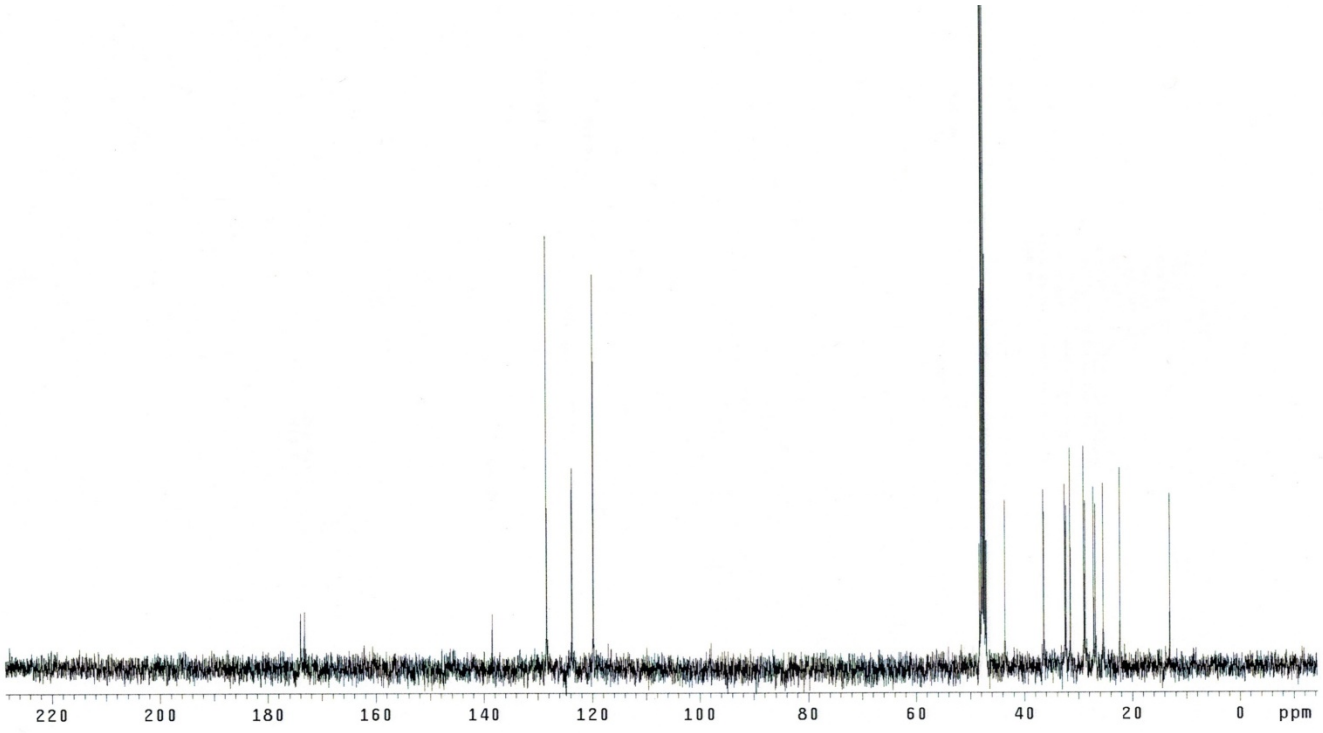

Figure S37: ^{13}C NMR spectrum of S-C2-*n*-hexyl SAHA (**S-1i**)

Elemental Composition Report **Page 1**

Single Mass Analysis
Tolerance = 5.0 PPM / DBE: min = -1.5, max = 100.0
Element prediction: Off
Number of isotope peaks used for i-FIT = 6

Monoisotopic Mass, Even Electron Ions
619 formula(e) evaluated with 1 results within limits (all results (up to 1000) for each mass)
Elements Used:
C: 20-20 H: 0-50 N: 0-50 O: 0-50 Na: 0-1

AN R_C2hexyl 12-08-2016 (V) 50
5

LCT Premier KD128
TOF MS ES+

1.43e+004

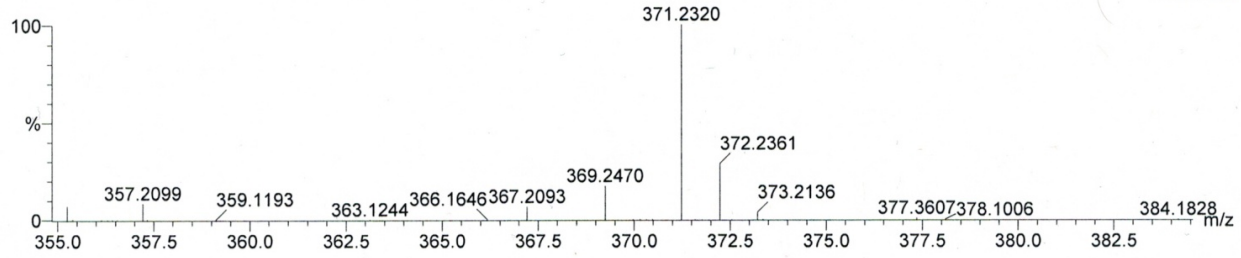

Minimum:				-1.5			
Maximum:		3.0	5.0	100.0			
Mass	Calc. Mass	mDa	PPM	DBE	i-FIT	i-FIT (Norm)	Formula
371.2320	371.2311	0.9	2.4	5.5	54.7	0.0	C20 H32 N2 O3 Na

Figure S38: High resolution mass spectrum of S-C2-*n*-hexyl SAHA (S-**1i**).

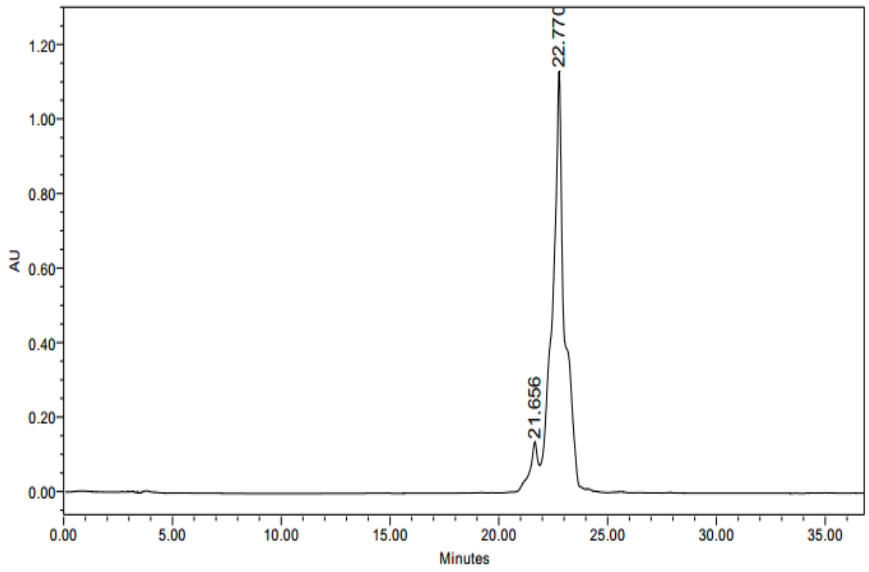

	RT	Area	% Area	Height
1	21.656	3653301	7.78	136293
2	22.770	43293512	92.22	1131343

Figure S39. HPLC spectrum taken at 254 nm of S-C2-*n*-hexyl SAHA (**S-1h**). The calculated area and height under each peak, along with % area, is shown in the table below the spectrum.

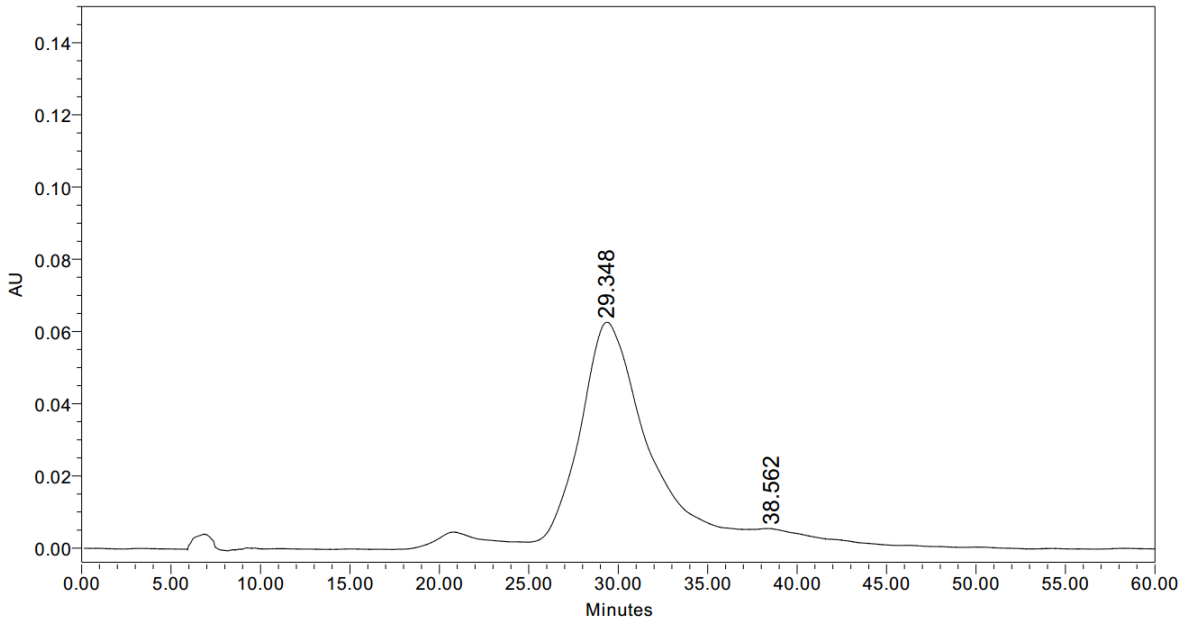

	RT	Area	% Area	Height
1	29.348	13214165	98.77	58447
2	38.562	163917	1.23	1143

Figure S40. Chiral HPLC spectrum of the (*S*)-C2-*n*-hexyl SAHA (***S*-1i**) taken at 254 nm. The major peak (29.3 min) represents the *S* enantiomer, while the minor peak (38.6 min) represents the *R* enantiomer (see Figure S11). The calculated area and height under each peak, along with % area, is shown in the table below the spectrum.

Supporting Figures and Tables:

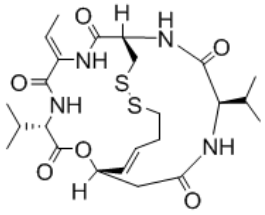

FK-228 (Romidepsin, Istodax™)

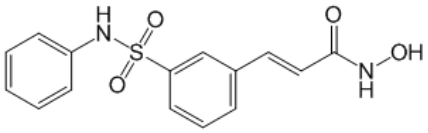

Belinostat (PXD101, Belodaq™)

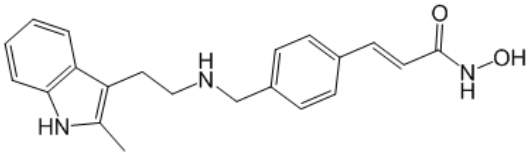

Panobinostat (LBH-589, Farydak™)

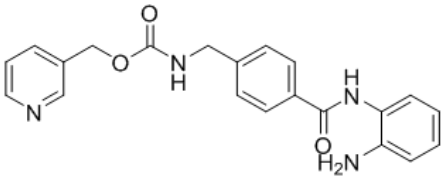

Entinostat (MS-275) (HDAC1, 2, 3 selective)

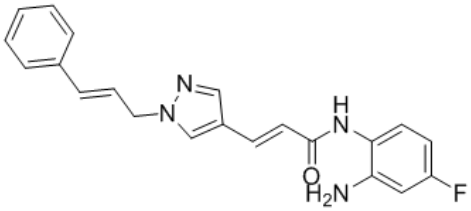

RGFP966 (HDAC3 selective)

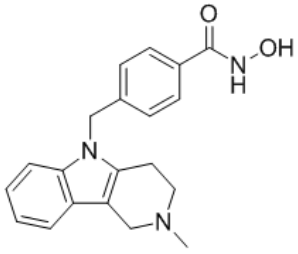

Tubastatin (HDAC6 selective)

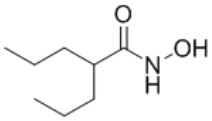

Valpropylhydroxamic acid (HDAC6/8 selective)

Figure S41: Chemical structures of the FDA approved HDAC inhibitors for cancer treatment and some isoform selective HDAC inhibitors mentioned in the introduction.

III. *In-vitro* HDAC activity screening data

Table S1: IC_{50} values for SAHA, and C2-modified SAHA analogs (**1a**-**1f**) with Hela cell lysates.[a]

Compound	R	IC_{50} (μM)
SAHA		0.090 ± 0.004
1a	methyl	134 ± 6
1b	ethyl	449 ± 17
1c	*n*-propyl	154 ± 7
1d	*n*-butyl	72 ± 6
1e	allyl	144 ± 9
1f	propargyl	87 ± 5
1g	benzyl	226 ± 11

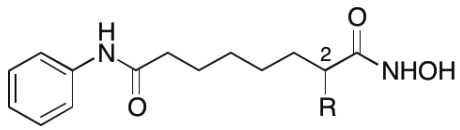

C_2-modified SAHA analogs

[a] Data are the mean and standard error, which were reported in an earlier publication.[8]

Table S2: Percent remaining deacetylase activity after incubation of a single concentration of SAHA and each C2-modified SAHA analog with HDAC1, HDAC2, HDAC3, and HDAC6 using the ELISA-based activity assay.[a]

	Deacetylase activity (%)			
compound	HDAC1	HDAC2	HDAC3	HDAC6
SAHA[2]	8.9±0.1	8.3±0.2	14±3	7.9±1.6
1a (methyl)	62±8	78±3	96±4	55±6
1b (ethyl)	76±5	65±6	88±5	52±6
1c (propyl)	75±4	69±1	86±7	49±5
1d (butyl)	69±8	82±4	78±6	39±4
1e (allyl)	83±6	78±3	90±3	52±7
1f (propargyl)	90±7	91±2	99±3	62±7
1g (benzyl)	92±4	99±1	92±8	30±6
1h (pentyl)	89±1	99±2	95±4	21±5
1i (hexyl)	91±4	98±1	100±3	26±2

[a] The means and standard errors for a minimum of three independent trials are shown. All analogs were used at 5μM final concentration, except SAHA and C2-butyl (**1d**) which were tested at 1μM and 10μM respectively. This data is associated with Figure 2 of the manuscript.

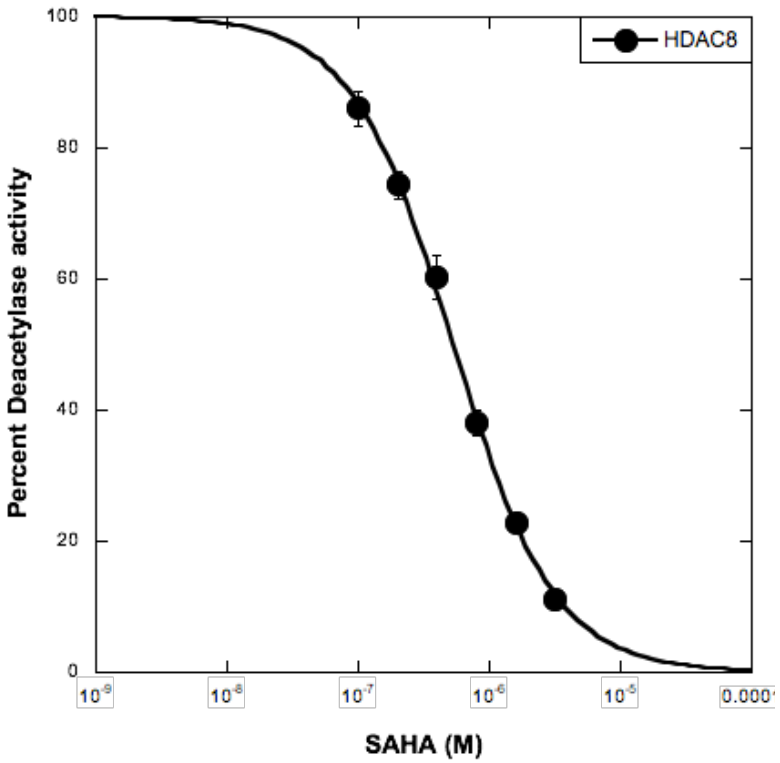

Figure S42: Dose dependent curve of SAHA with HDAC8 isoform with error bars depicting the standard error of at three independent trials. In some cases, the error bars are smaller than the size of the filled circle. IC_{50} values associated with Table 1 of manuscript were determined by fitting data to a sigmoidal curve using Kaleidograph 4.1.3 (Synergy Software) (Table S3).

Table S3: Percentage remaining deacetylase activity after incubation of SAHA with HDAC8.[a]

Concentration (M)	Deacetylase activity (%)
3.2×10^{-6}	11±1
1.6×10^{-6}	23±1
8.0×10^{-7}	38±2
4.0×10^{-7}	60±3
2.0×10^{-7}	74±2
1.0×10^{-7}	86±3

[a] Means and standard errors of at three independent trials with the SAHA concentrations shown. Data is associated with Figure S42 and Table 1 of the manuscript.

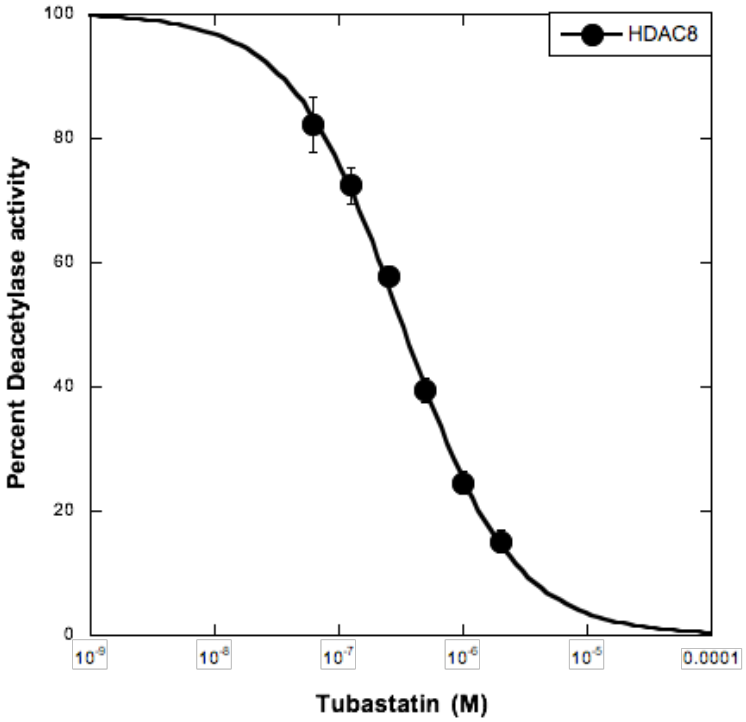

Figure S43: Dose dependent curve of Tubastatin with HDAC8 isoform with error bars depicting the standard error of at three independent trials. In some cases, the error bars are smaller than the size of the filled circle. IC_{50} values associated with Table 1 of manuscript were determined by fitting data to a sigmoidal curve using Kaleidograph 4.1.3 (Synergy Software) (Table S4).

Table S4: Percentage remaining deacetylase activity after incubation of Tubastatin with HDAC8.[a]

Concentration (M)	Deacetylase activity (%)
2.0×10^{-6}	15±2
1.0×10^{-6}	25±2
5.0×10^{-7}	40±2
2.5×10^{-7}	58±1
1.25×10^{-7}	73±3
6.25×10^{-8}	82±4

[a] Means and standard errors of at three independent trials with the Tubastatin concentrations shown. Data is associated with Figure S43 and Table 1 of the manuscript.

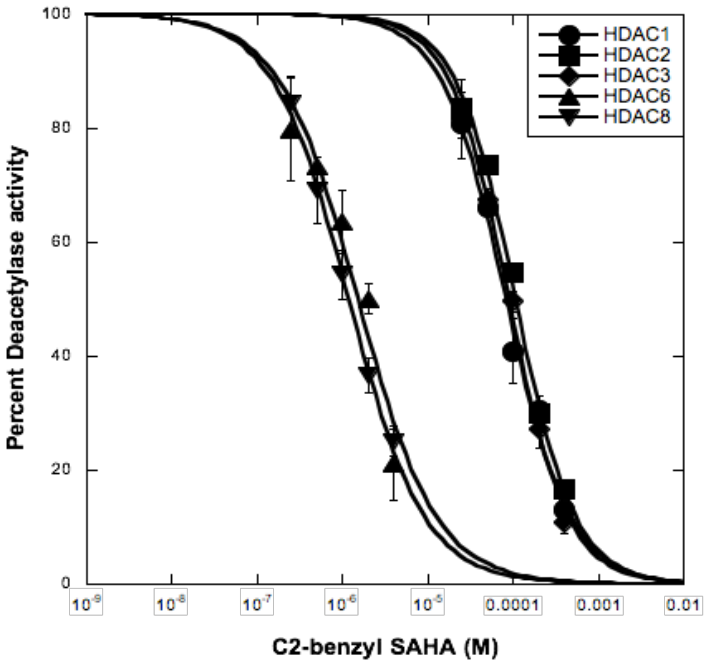

Figure S44: Dose dependent curves of C2-benzyl SAHA analog (**1g**) with HDAC1, HDAC2, HDAC3, HDAC6, and HDAC8 isoforms with error bars depicting the standard error of at least two independent trials. IC_{50} values associated with Table 1 of manuscript were determined by fitting data to a sigmoidal curve using Kaleidograph 4.1.3 (Synergy Software) (Table S5).

Table S5: Percentage remaining deacetylase activity after incubation of C2-benzyl SAHA (**1g**) with HDAC1, HDAC2, HDAC3, HDAC6, and HDAC8.[a]

Concentration (M)	Deacetylase activity (%)				
	HDAC1	HDAC2	HDAC3	HDAC6	HDAC8
4.0×10^{-4}	13±1	17±1	11±2		
2.0×10^{-4}	31±2	30±2	27±3		
1.0×10^{-4}	41±6	55±1	50±2		
5.0×10^{-5}	66±1	74±1	68±2		
2.5×10^{-5}	81±3	84±3	82±7		
4.0×10^{-6}				21±7	25±2
2.0×10^{-6}				50±3	37±3
1.0×10^{-6}				64±6	54±4
5.0×10^{-7}				73±1	69±6
2.5×10^{-7}				80±9	84±5

[a] Means and standard errors of at least two independent trials with the C2-benzyl SAHA (**1g**) concentrations shown. Data is associated with Figure S44 and Table 1 of the manuscript.

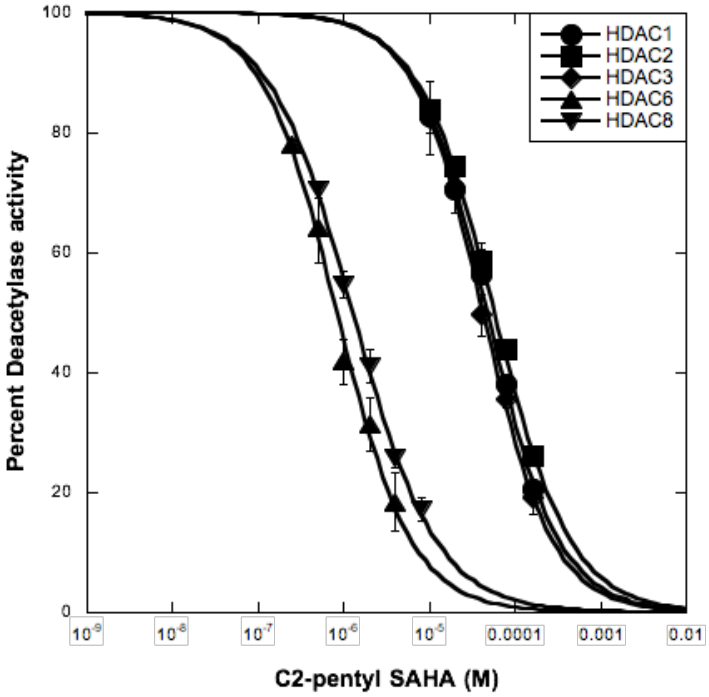

Figure S45: Dose dependent curves of C2-*n*-pentyl SAHA analog (**1h**) with HDAC1, HDAC2, HDAC3, HDAC6, and HDAC8 isoforms with error bars depicting the standard error of at least two independent trials. IC_{50} values associated with Table 1 of manuscript were determined by fitting data to a sigmoidal curve using Kaleidograph 4.1.3 (Synergy Software) (Table S6).

Table S6: Percentage remaining deacetylase activity after incubation of C2-*n*-pentyl SAHA (**1h**) with HDAC1, HDAC2, HDAC3, HDAC6, and HDAC8.[a]

Concentration (M)	Deacetylase Activity (%)				
	HDAC1	HDAC2	HDAC3	HDAC6	HDAC8
1.6×10^{-4}	21±1	26±1	19±3		
8.0×10^{-5}	38±1	44±1	36±2		
4.0×10^{-5}	56±4	59±3	50±3		
2.0×10^{-5}	71±1	74±1	71±4		
1.0×10^{-5}	83±3	84±1	83±6		
8.0×10^{-6}					17±2
4.0×10^{-6}				18±5	26±1
2.0×10^{-6}				31±4	41±3
1.0×10^{-6}				42±4	55±2
5.0×10^{-7}				64±6	71±1
2.5×10^{-7}				78±1	

[a] Means and standard errors of at least two independent trials with the C2-*n*-pentyl SAHA (**1h**) concentrations shown. Data is associated with Figure S45 and Table 1 of the manuscript.

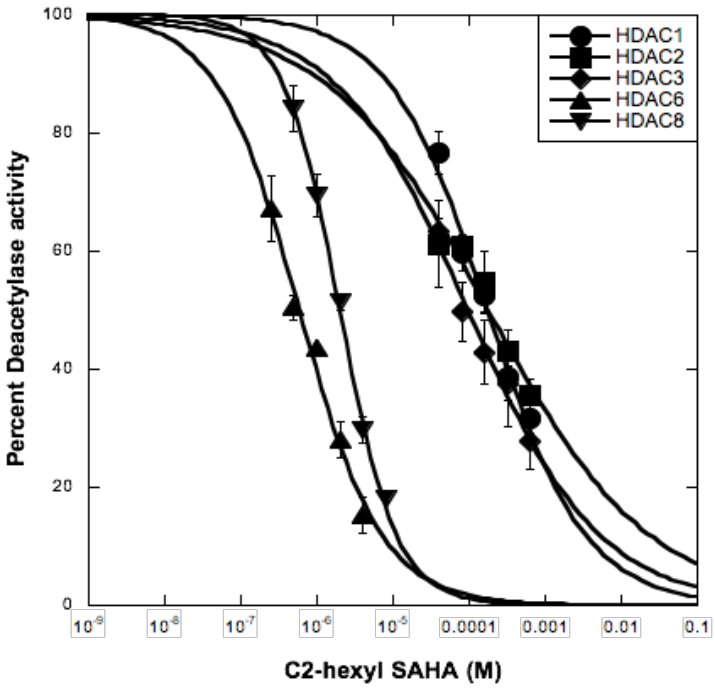

Figure S46: Dose dependent curves of C2-*n*-hexyl SAHA derivative (**1i**) with HDAC1, HDAC2, HDAC3, HDAC6, and HDAC8 isoforms with error bars depicting the standard error of at least two independent trials. IC_{50} values associated with Table 1 of manuscript were determined by fitting data to a sigmoidal curve using Kaleidograph 4.1.3 (Synergy Software) (Table S7).

Table S7: Percentage of remaining HDAC deacetylase activity after incubation of C2-*n*-hexyl SAHA derivative (**1i**) HDAC1, HDAC2, HDAC3, HDAC6, and HDAC8.[a]

Concentration (M)	Deacetylase Activity (%)				
	HDAC1	HDAC2	HDAC3	HDAC6	HDAC8
6.4×10^{-4}	32±2	35±3	28±5		
3.2×10^{-4}	39±8	43±1	38±3		
1.6×10^{-4}	52±3	55±5	43±5		
8.0×10^{-5}	60±3	61±2	50±5		
4.0×10^{-5}	77±4	61±7	63±2		
8.0×10^{-6}					18±1
4.0×10^{-6}				15±3	30±2
2.0×10^{-6}				28±3	51±1
1.0×10^{-6}				44±1	70±4
5.0×10^{-7}				50±2	84±4
2.5×10^{-7}				67±6	

[a] Means and standard errors of at least two independent trials are shown. Data is associated with Figure S46 and Table 1 of the manuscript.

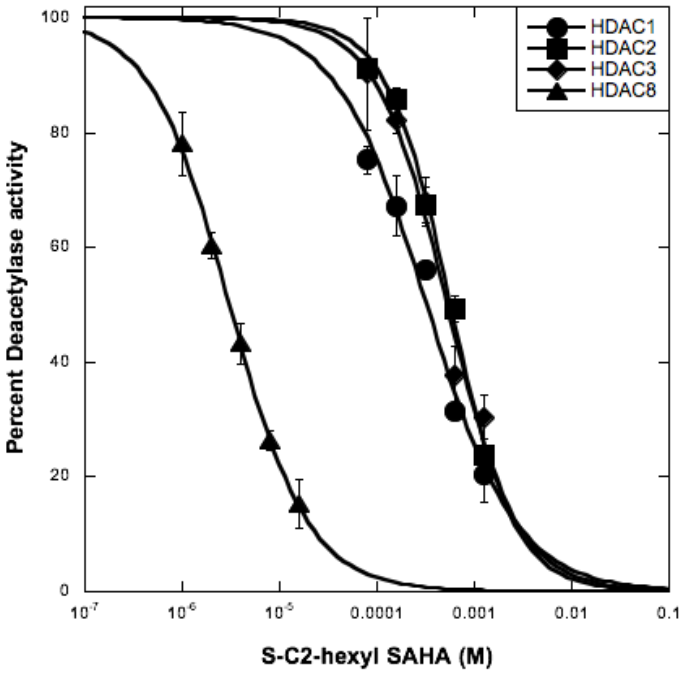

Figure S47: Dose dependent curves of (S)-C2-*n*-hexyl SAHA derivative (**1i**) with HDAC1, HDAC2, HDAC3, and HDAC8 isoforms with error bars depicting the standard error of at least two independent trials. IC_{50} values associated with Table 1 of manuscript were determined by fitting data to a sigmoidal curve using Kaleidograph 4.1.3 (Synergy Software) (Table S8).

Table S8: Percentage of remaining HDAC deacetylase activity after incubation of C2-*n*-hexyl SAHA derivative (**1i**) HDAC1, HDAC2, HDAC3, and HDAC8.[a]

Concentration (M)	Deacetylase Activity (%)			
	HDAC1	HDAC2	HDAC3	HDAC8
1.28×10^{-3}	20±5	24±1	30±4	
6.4×10^{-4}	32±1	49±2	38±5	
3.2×10^{-4}	56±1	68±3	68±4	
1.6×10^{-4}	67±5	86±2	82±2	
8.0×10^{-5}	75±2	91±1	90±10	
1.6×10^{-5}				15±4
8.0×10^{-6}				26±2
4.0×10^{-6}				43±4
2.0×10^{-6}				60±2
1.0×10^{-6}				78±6

[a] Means and standard errors of at least two independent trials are shown. Data is associated with Figure S47 and Table 1 of the manuscript.

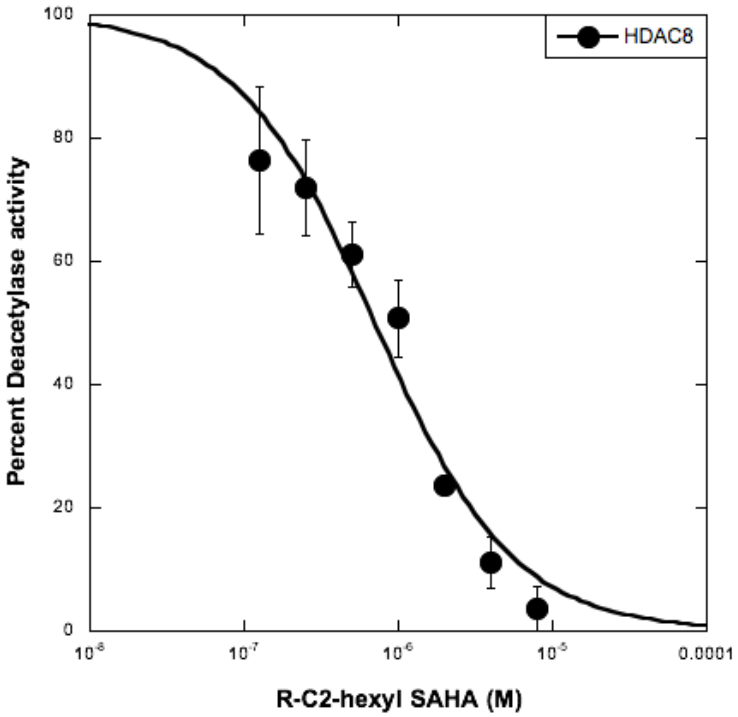

Figure S48: Dose dependent curves of (R)-C2-*n*-hexyl SAHA derivative (**1i**) with HDAC8 isoform with error bars depicting the standard error of at least two independent trials. IC_{50} values associated with Table 1 of manuscript were determined by fitting data to a sigmoidal curve using Kaleidograph 4.1.3 (Synergy Software) (Table S9).

Table S9: Percentage of remaining HDAC deacetylase activity after incubation of (R)-C2-*n*-hexyl SAHA derivative and HDAC8.[a]

Concentration (M)	Deacetylase Activity (%)
	HDAC8
8.0×10^{-6}	3.7±3.5
4.0×10^{-6}	11±4
2.0×10^{-6}	24±1
1.0×10^{-6}	50±6
5.0×10^{-7}	63±5
2.5×10^{-7}	72±8
1.25×10^{-7}	76±12

[a] Means and standard errors of at least two independent trials are shown. Data is associated with Figure S48 and Table 2 of the manuscript.

IV. In cell selectivity data

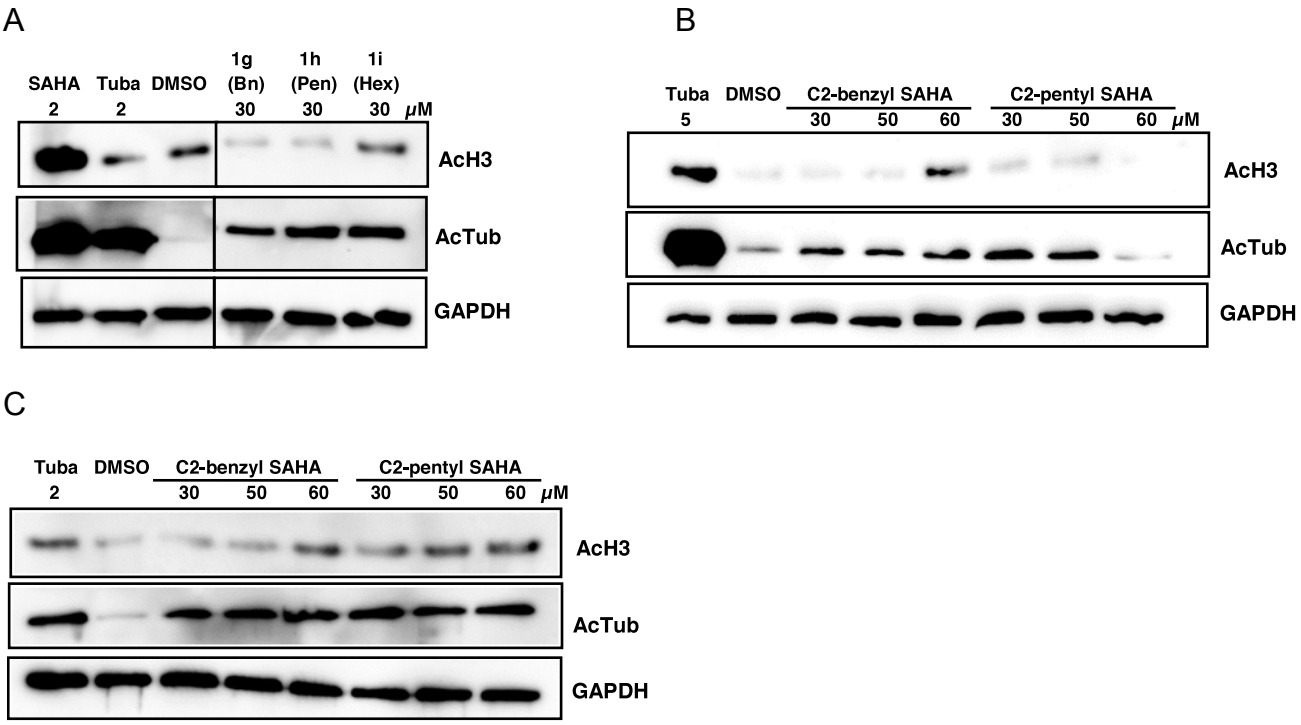

Figure S49: Representative cell-based selectivity trials with SAHA, Tubastatin and SAHA analogs. U937 cells were treated with DMSO (1%), SAHA, C2-benzyl SAHA (**1g**), C2-n-pentyl SAHA (**1h**), C2-n-hexyl SAHA (**1i**). After lysis and SDS-PAGE separation of the proteins in the lysates, western blots analysis of acetyl-histone H3 (AcH3) and acetyl-α-tubulin (AcTub) was performed. GAPDH was used as a loading control. DMSO was used as the no inhibitor control. These three trials (parts A-C) are associated with the fourth trial shown in Figure 3a of the manuscript.

Table S10: Fold increase in acetyl-histone H3 and acetyl-tubulin at 30 μM of SAHA analogs **1g, 1i,** and **1h**, compared to DMSO treated cells for the western blots images in figures 3a and S46.[a]

Compound	Acetyl-histone H3		Acetyl-tubulin	
	Mean fold increase	Standard error	Mean fold increase	Standard error
1g (beznyl)	0.99	0.32	5.002862	0.797345
1i (pentyl)	1.59	0.84	7.482278	3.199188
1h (hexyl)	1.32	0.44	3.937545	0.529507

[a] Means and standard errors of three independent trials are shown. Data is associated with Figures 3a and S49.

A

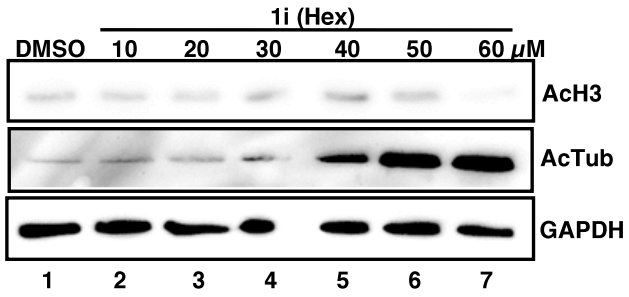

B

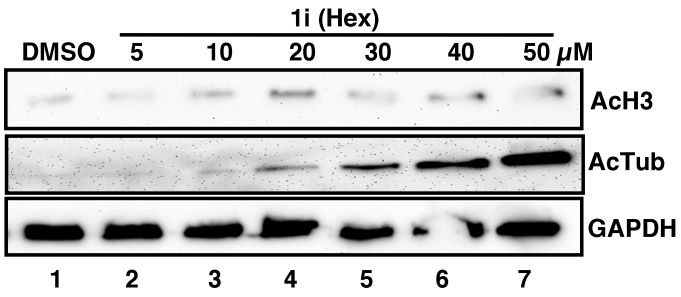

Figure S50: Repetitive cell-based selectivity trials with C2-n-hexyl SAHA analog (1i). U937 cells were treated with increasing concentrations of C2-n-hexyl SAHA analog (**1i**, 10-60 μM or 5-50 μM). After lysiss and SDS-PAGE separation of the proteins in the lysates, western blot analysis of acetyl-histone H3 (AcH3) and acetyl-α-tubulin (AcTub) was performed. GAPDH was used as a loading control. DMSO was used as the no inhibitor control. These two trials (parts A and B) are associated with the third trial shown in Figure 3b of the manuscript.

V. Cell growth inhibition data

Table S11: Percentage of viable cells after treatment of Jurkat cell line with of C2-benzyl SAHA **1g**, C2-pentyl SAHA **1h**, C2-hexyl SAHA **1i**, and SAHA.[a]

	Viable cells (%)	
Compound	1 μM	10 μM
1g (benzyl)	100 ± 8	83 ± 2
1h (pentyl)	80 ± 13	92 ± 8
1i (hexyl)	88 ± 11	47 ± 9
SAHA	49 ± 6	5 ± 3

[a] Means and standard errors for a minimum of three independent trials are shown. All analogs were tested at 1 and 10μM final concentrations. Data is associated with Figure 4 from manuscript.

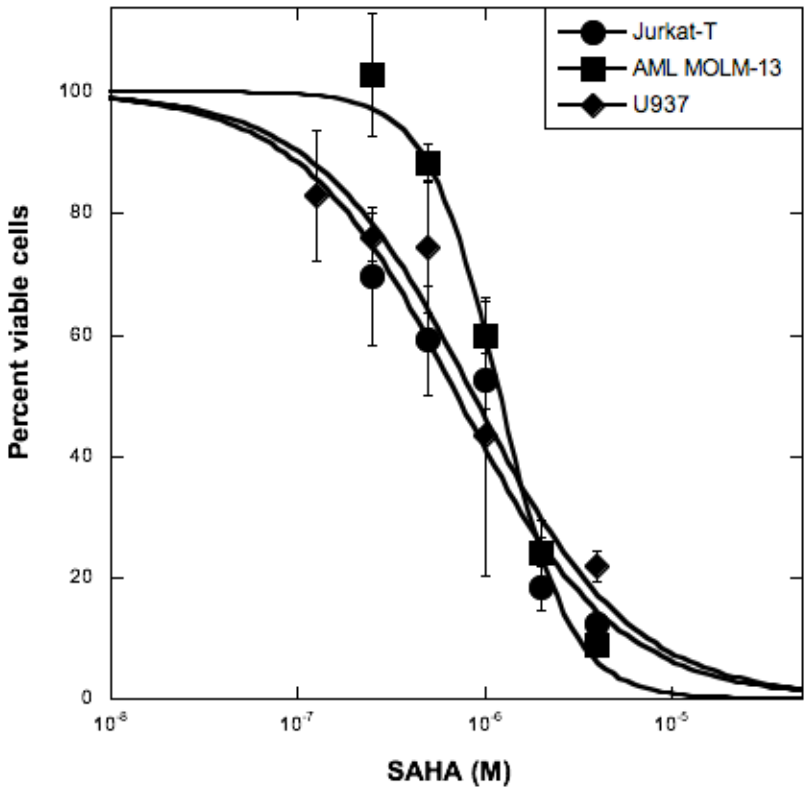

Figure S51: Dose dependent cell viability of SAHA with Jurkat, AML MOLM-13, and U937 cell lines, with error bars depicting the standard error of at least three independent trials. EC_{50} values associated with Table 2 of manuscript were determined by fitting data to a sigmoidal curve using Kaleidagraph 4.1.3 (Synergy Software) (Table S12).

Table S12: Percentage of viable cells after treatment of different cell lines with SAHA at the specified concentrations.[a]

Concentration (M)	Viable cells (%)		
	Jurkat	AML-MOL13	U937
4.0×10^{-6}	12 ± 1	9 ± 1	22 ± 3
2.0×10^{-6}	18 ± 4	24 ± 2	24 ± 6
1.0×10^{-6}	53 ± 5	60 ± 6	43 ± 23
5.0×10^{-7}	59 ± 9	88 ± 3	75 ± 11
2.5×10^{-7}	70 ± 11	103 ± 10	76 ± 4
1.25×10^{-7}			83 ± 11

[a] Standard errors of at least three independent trials are shown. Data is associated with Figure S51 and Table 2 of the manuscript.

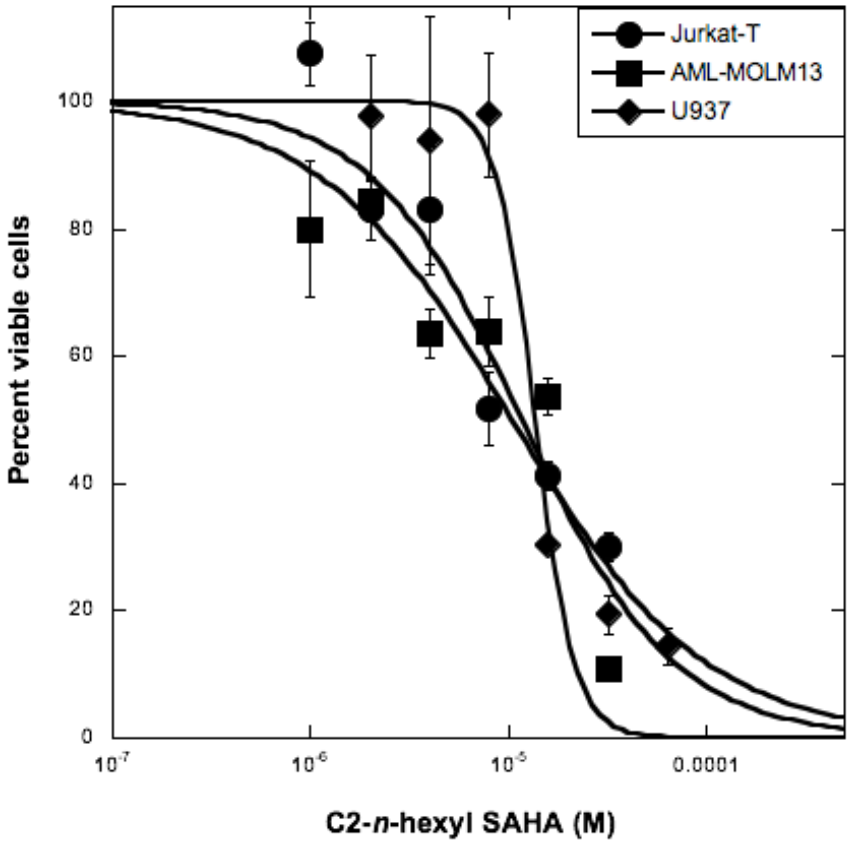

Figure S52: Dose dependent cell viability of C2-*n*-hexyl SAHA (**1i**) with Jurkat, AML MOLM-13, and U937 cell lines, with error bars depicting the standard error of more than three independent trials. EC_{50} values associated with Table 2 of manuscript were determined by fitting data to a sigmoidal curve using KaleidaGraph 4.1.3 (Synergy Software) (Table S13).

Table S13: Percentage of viable cells after treatment of different cell lines with of C2-*n*-hexyl SAHA (**1i**) at the specified concentrations.[a]

Concentration (M)	Viable cells (%)		
	Jurkat	AML-MOL13	U937
6.4×10^{-5}			14 ± 3
3.2×10^{-5}	30 ± 2	11 ± 1	19 ± 3
1.6×10^{-5}	41 ± 2	54 ± 3	30 ± 1
8.0×10^{-6}	52 ± 6	64 ± 5	98 ± 10
4.0×10^{-6}	83 ± 10	64 ± 4	94 ± 20
2.0×10^{-6}	83 ± 5	84 ± 3	98 ± 10
1.0×10^{-6}	108 ± 5	80 ± 11	

[a] Means and standard errors of at least three independent trials are shown. Data is associated with Figure S52 and Table 2 of the manuscript.

VI. Docking figures

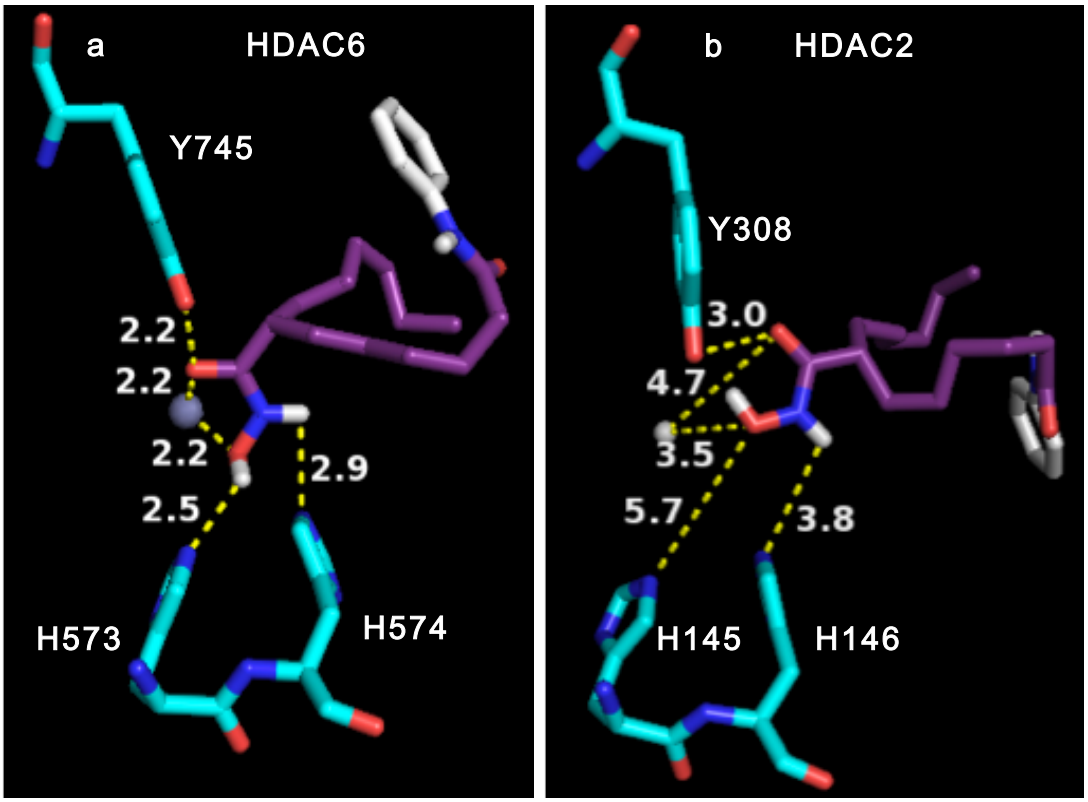

Figure S53: Docked poses of (*R*)-C2-*n*-hexyl SAHA ((*R*)-**1i**) in the (A) HDAC6 (pdb:5EEM)[6] and the HDAC2 (pdb:3MAX)[5] crystal structure (**B**) using Autodock 4.2.[4] Binding distances between the hydroxamic acid atoms and active site residues (numbered in figure) or the metal are displayed in Angstroms. The atomic radii of the metals were set at 0.5 Å for clarity. Atom color-coding: (R)-C2-*n*-hexyl SAHA (C=purple/white; O=red; N=blue; H=white); amino acids (C=deep teal; O=red, N=blue); Zn^{2+} metal ion (grey sphere).

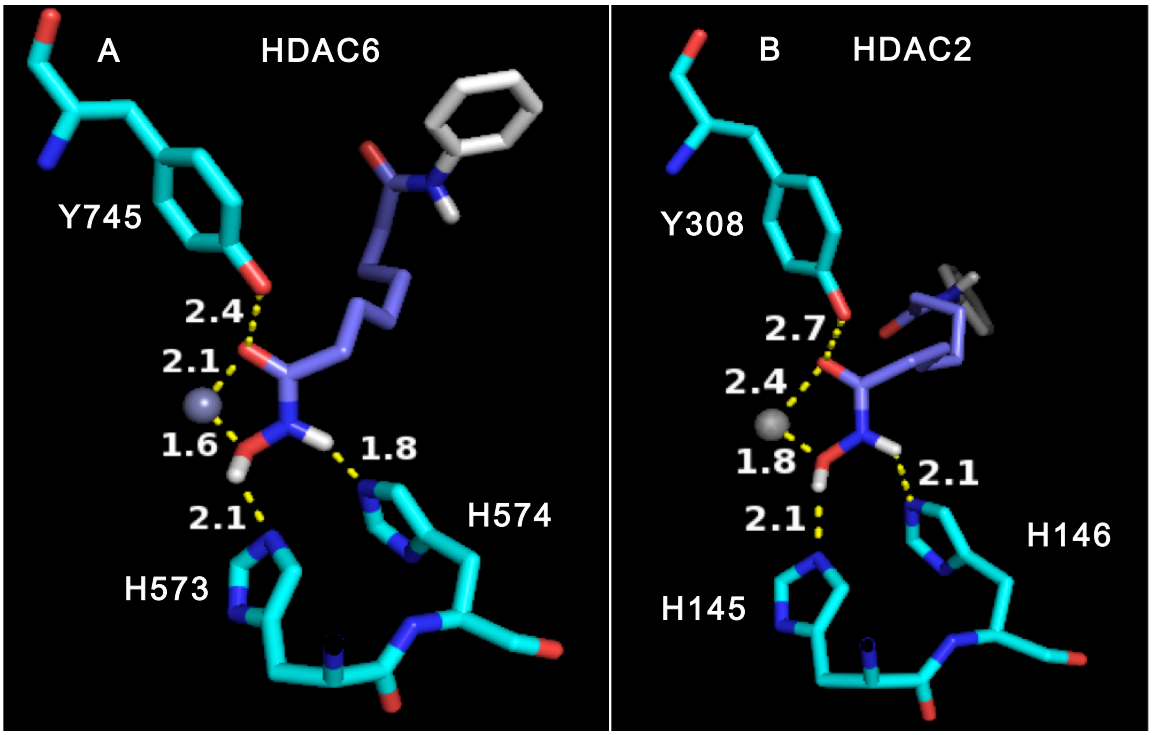

Figure S54: Docking poses of SAHA in the (A) HDAC6 (pdb:5EEM)[6] or (B) HDAC2 (pdb:3MAX)[5] crystal structures and using Autodock 4.2.[4] Binding distances between the hydroxamic acid atoms and active site residues (numbered in figure) or the metal are displayed in Angstroms. The atomic radii of the metals were set at 0.5 Å for clarity. Color-coded SAHA (C=purple/white; O=red; N=blue; H=white) and amino acid residues (C=deep teal; O=red, N=blue); Zn^{2+} metal ion (grey sphere).

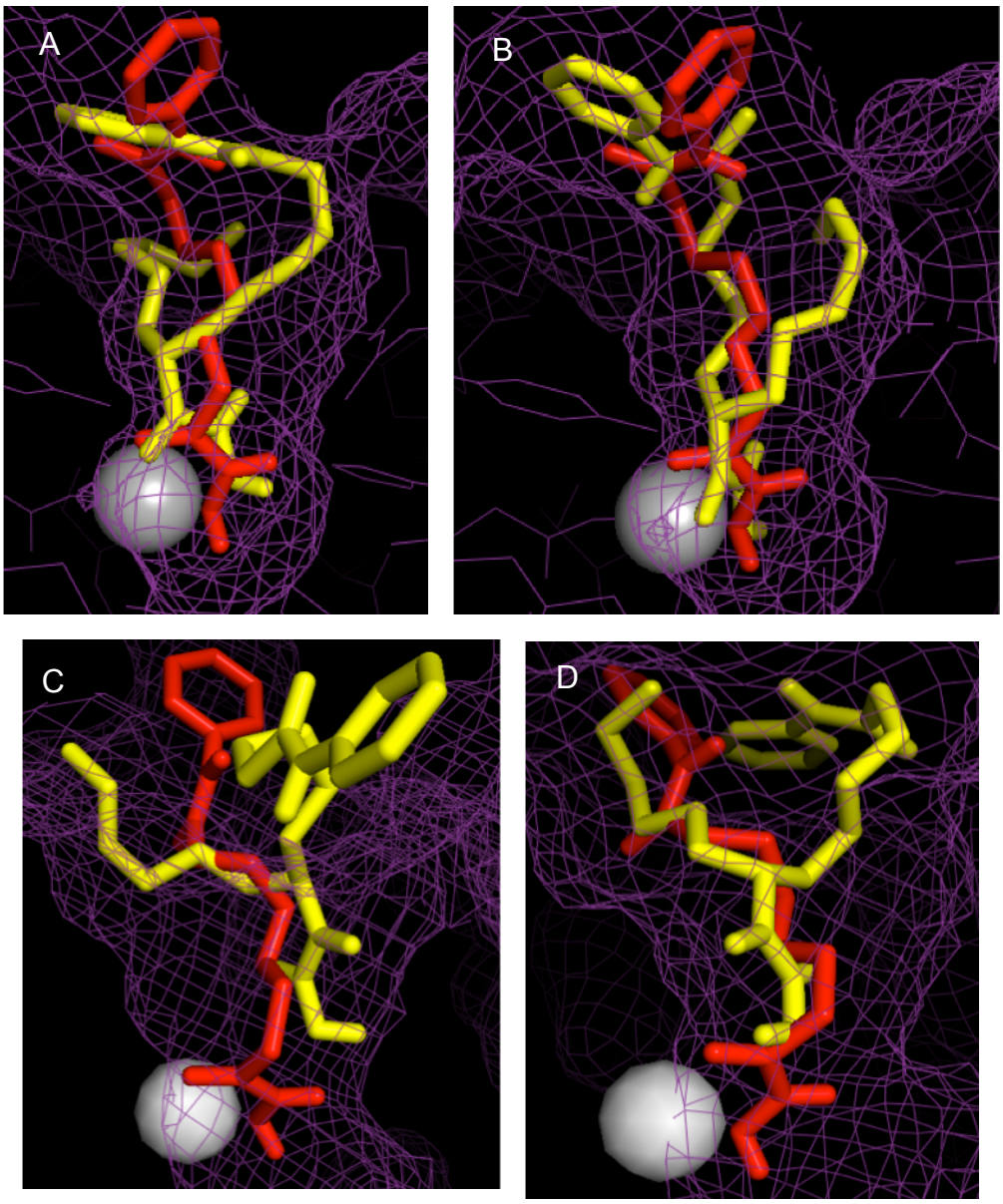

Figure S55. Superimposition of SAHA (red) and either (R)-C2-n-hexyl SAHA 1i (A and C) or (S)-C2-n-hexyl SAHA 1i (B and D) (yellow) in the HDAC6 (A and B) (pbd:5EEM) or HDAC2 (C and D) (pbd:3MAX) crystal structures), with the metal ion (Zn^{2+}) represented as a grey sphere (1.35 Å radius). Notice that the metal sphere is in close proximity to the hydroxamic acid end of both SAHA and the analogs in the HDAC6 sturctures. In contrast, the analogs are positioned farther from the metal sphere than SAHA, consistent with the poor potency observed.

VII. References

(1) Bonnett, S. A.; Papireddy, K.; Higgins, S.; del Cardayre, S.; Reynolds, K. A., Functional Characterization of an NADPH Dependent 2-Alkyl-3-ketoalkanoic Acid Reductase Involved in Olefin Biosynthesis in Stenotrophomonas maltophilia. *Biochemistry* **2011,** *50* (44), 9633-9640.

(2) Blagosklonny, M. V.; Robey, R.; Sackett, D. L.; Du, L.; Traganos, F.; Darzynkiewicz, Z.; Fojo, T.; Bates, S. E., Histone deacetylase inhibitors all induce p21 but differentially cause tubulin acetylation, mitotic arrest, and cytotoxicity. *Molecular cancer therapeutics* **2002,** *1* (11), 937-41.

(3) Sanner, M. F., Python: a programming language for software integration and development. *Journal of molecular graphics & modelling* **1999,** *17* (1), 57-61.

(4) Morris, G. M.; Huey, R.; Lindstrom, W.; Sanner, M. F.; Belew, R. K.; Goodsell, D. S.; Olson, A. J., AutoDock4 and AutoDockTools4: automated docking with selective receptor flexibility. *Journal of computational chemistry* **2009,** *30* (16), 2785-2791.

(5) Bressi, J. C.; Jennings, A. J.; Skene, R.; Wu, Y.; Melkus, R.; De Jong, R.; O'Connell, S.; Grimshaw, C. E.; Navre, M.; Gangloff, A. R., Exploration of the HDAC2 foot pocket: Synthesis and SAR of substituted N-(2-aminophenyl)benzamides. *Bioorganic & medicinal chemistry letters* **2010,** *20* (10), 3142-5.

(6) Hai, Y.; Christianson, D. W., Histone deacetylase 6 structure and molecular basis of catalysis and inhibition. *Nat Chem Biol* **2016,** *12* (9), 741-747.

(7) Gottlieb, H. E.; Kotlyar, V.; Nudelman, A., NMR Chemical Shifts of Common Laboratory Solvents as Trace Impurities. *The Journal of organic chemistry* **1997,** *62* (21), 7512-7515.

(8) Bieliauskas, A.; Weerasinghe, S.; Pflum, M. H., Structural requirements of HDAC inhibitors: SAHA analogs functionalized adjacent to the hydroxamic acid. *Bioorg. Med. Chem. Lett.* **2007,** *17* (8), 2216-2219.